

doi: [10.12097/gbc.2024.04.046](https://doi.org/10.12097/gbc.2024.04.046)

赣南上洞变玄武岩矿物学、地球化学特征及其成因

马玉香, 刘帅*, 杜后发, 姚玥, 赵亮

MA Yuxiang, LIU Shuai*, DU Houfa, YAO Yue, ZHAO Liang

东华理工大学地球科学学院, 江西 南昌 330013

School of Earth Sciences, East China University of Technology, Nanchang 330013, Jiangxi, China

摘要:【研究目的】最新在赣南上洞发现的变玄武岩位于华夏加里东褶皱带南缘, 对其成因和形成构造环境研究, 可为解释华南加里东褶皱带构造属性提供依据。【研究方法】以上洞变玄武岩为研究对象, 进行了矿物学、地球化学特征研究。【研究结果】上洞变玄武岩的主要组成矿物为角闪石、斜长石、辉石和黑云母; 全岩地球化学分析显示, 变玄武岩属于亚碱性拉斑玄武岩系列, 具有中等 $Mg^{\#}$ (40.44~45.16)、富钠贫钾($K_2O/Na_2O=0.07\sim0.16$), 轻稀土元素中等富集, 无显著 Eu 异常($Eu=1.03\sim1.11$), 富 Nb、显著的 Sr-Nb-Ta 弱亏损特征。矿物学研究显示, 辉石具富镁、富钙的特点, 属普通辉石, 结晶温度 1184°C; 黑云母为铁质黑云母, 结晶温度 660°C, 具有富铝、富铁, 贫镁、贫钾的特点; 角闪石具贫钛、富钙、富铁、富铝的特点, 属钙质闪石组中的普通角闪石, 结晶温度 594°C; 斜长石具贫钛、富钠、富铝的特点, 属于中长石-奥长石。【结论】研究表明, 赣南上洞变玄武岩形成于高温、高氧逸度的环境, 属于壳幔混源的玄武质岩浆, 具有岛弧环境特征, 暗示华南早古生代加里东期构造背景应属于俯冲背景。

关键词:变玄武岩; 矿物学; 地球化学; 岩石成因; 赣南上洞

创新点:首次在华夏地块南缘发现具有典型岛弧特征的变玄武岩, 通过系统的矿物学和地球化学研究, 揭示其形成于俯冲相关的构造环境, 为华南早古生代加里东期造山作用提供了关键的岩浆岩证据。

中图分类号: P575; P595 文献标志码: A 文章编号: 1671-2552(2025)05-0902-19

Ma Y X, Liu S, Du H F, Yao Y, Zhao L. Mineralogical, geochemical characteristics, and genesis of Shangdong meta-basalt in Southern Jiangxi. *Geological Bulletin of China*, 2025, 44(5): 902–920

Abstract: [Objectives] The recently discovered meta-basalt in Shangdong, southern Jiangxi Province, is situated at the southern margin of the Cathaysia Caledonian fold belt. Investigating its petrogenesis and tectonic setting of formation is crucial for elucidating the tectonic nature of the South China Caledonian fold belt. [Methods] This study focuses on the Shangdong meta-basalt, employing a comprehensive approach combining mineralogical observations and detailed geochemical analyses to constrain its geological history. [Results] Mineralogical examination reveals that the Shangdong meta-basalt is primarily composed of hornblende, plagioclase, pyroxene, and biotite. Geochemical data indicate that it belongs to the sub-alkaline tholeiite series, characterized by moderate $Mg^{\#}$ values (40.44~45.16), a distinct Na-rich/K-poor signature ($K_2O/Na_2O=0.07\sim0.16$), moderate enrichment of light rare earth elements, negligible Eu anomalies ($Eu=1.03\sim1.11$), and notable depletion in Sr, Nb, and Ta despite relative Nb enrichment. Mineral-specific analyses further demonstrate that pyroxene is a Mg-Ca-rich augite with a crystallization temperature of 1184 °C; biotite is ferrobiotite, crystallizing at 660 °C and exhibiting high Al and Fe contents with low Mg and K; hornblende is a Ca-rich, Ti-poor, Fe-Al-enriched common hornblende within the calcic amphibole group, crystallizing at 594°C; and plagioclase is a Ti-poor, Na-Al-rich andesine-oligoclase. [Conclusions] Collectively, these findings suggest that the Shangdong meta-basalt formed under high-temperature and high oxygen fugacity conditions, originating from a magma generated by crust-mantle mixing. Its geochemical and mineralogical features are indicative of an island arc tectonic setting, strongly implying that the South China region experienced a

收稿日期: 2024-04-24; 修订日期: 2024-06-18

资助项目: 国家自然科学基金项目《赣南-粤北相邻区河口-南迳加里东期火山岩研究与铀成矿关系》(批准号: 41662006)

作者简介: 马玉香(1999-), 女, 硕士, 从事地球化学研究。E-mail: 3517962405@qq.com

* 通信作者: 刘帅(1978-), 男, 博士, 教授, 从事矿产普查与勘探研究。E-mail: Liushuai7821@163.com

subduction-related tectonic regime during the Early Paleozoic Caledonian orogeny.

Key words: meta-basalt; mineralogy; geochemistry; petrogenesis; Shangdong in Southern Jiangxi

Highlights: The first discovery of meta-basalt with typical arc signatures in the southern margin of the Cathaysia Block, combined with systematic mineralogical and geochemical investigations, reveals their formation in a subduction-related tectonic setting, providing critical magmatic evidence for the Early Paleozoic Caledonian orogeny in South China.

华南加里东造山带位于扬子古板块和华夏古板块拼合汇聚部位 (Wang et al., 2006; Zheng et al., 2006; Li et al., 2009; 舒良树等, 2012; Zhang and Zheng, 2013; 高彭, 2016)。针对加里东造山带的构造属性, 学者们进行了广泛研究, 观点分为2种:一种认为其为陆内造山, 另一种则认为是俯冲-碰撞造山。要解决这一争议, 关键在于是否存在同时期的岛弧火山岩和蛇绿岩作为关键性证据。徐克勤等(1960)首次在赣南上犹陡水和南康龙回地区发现早古生代花岗岩, 但由于缺乏同期火山岩、蛇绿岩、洋-陆俯冲活动大陆边缘等相关证据, 倾向认为该造山带具有陆内造山特征 (周新民, 2003; 王帅, 2004; 王德滋, 2004; Wang et al., 2007; 徐夕生, 2008; Li et al., 2010a; 关义立, 2013; 张国伟, 2013)。但随着在赣南—粤北地区陆续发现了加里东期碎斑熔岩 (443.6 ± 5.4 Ma)、英安(斑)岩 (448.7 ± 1.7 Ma)、安山岩 (442.1 ± 3.9 Ma)、流纹岩 (436 ± 2.4 Ma) 等火山岩, 从岩石学和地球化学研究结果看, 这些发现均指示了洋陆俯冲-碰撞的地质历程 (巫建华, 2012; 易立文, 2014; 伍静, 2014; 丁辉, 2016; 彭松柏等, 2016; 劳玉军, 2017; 马树松,

2019; 刘帅, 2020, 2021; 张山, 2021; 张素梅, 2024; 曹明轩等, 2025)。

本次发现的赣南上洞变玄武岩位于华夏加里东褶皱带南缘, 是研究华南岩浆活动、构造环境等地质问题的重要区域, 其岩石成因和形成构造环境尚未有相关研究报道。开展变玄岩成因和构造环境矿物学研究, 可为进一步研究华南加里东构造带构造属性提供新依据。本文以上洞变玄岩为研究对象, 通过岩相学、矿物学证据、地球化学研究, 探讨变玄武岩岩石成因和构造环境, 综合前人研究成果, 为揭示华南加里东造山带的构造属性、重新认识华南加里东期岩浆活动及构造背景提供新的参考。

1 大地构造背景

研究区大地构造位置上属于华南板块之华夏地块中东部 (图 1-a), 位于华夏加里东褶皱带南缘, 华夏加里东褶皱带与湘桂粤印支褶皱带的交会部位, 区域断裂构造处于北东向恩平-新丰-鹰潭大断裂带和北西向汕头-安仁大断裂带交会处 (图 1-b)。华夏地块主要由元古宙结晶基底构成, 包括武夷山北的

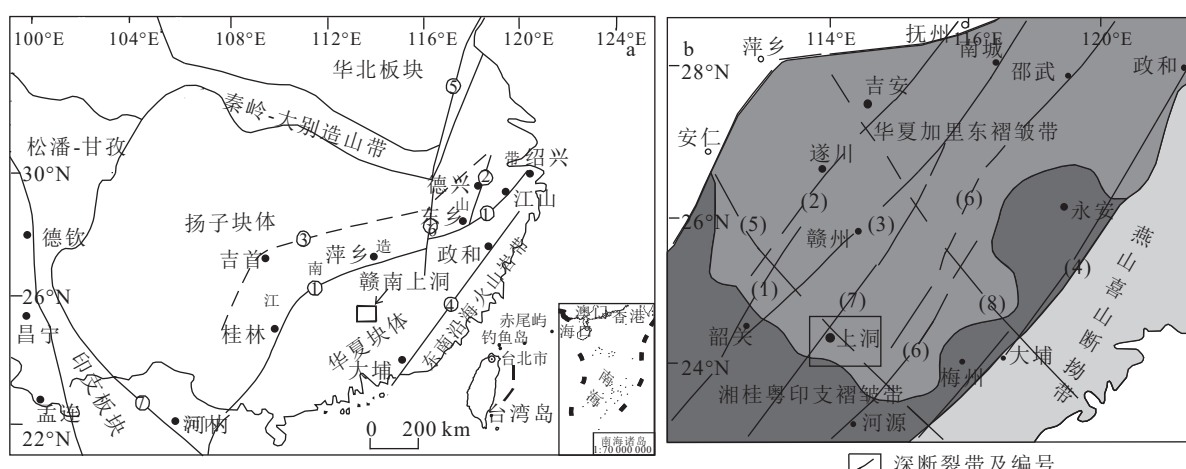


图 1 华南区域构造简图 (a, 据舒良树等, 2012) 和区域大地构造、深断裂分布图 (b, 据朱捌, 2010)

Fig. 1 Tectonic map of the South China (a) and distribution map of regional tectonic units and deep faults (b)

- ①—绍兴-江山-萍乡断裂带; ②—东乡-德兴断裂带; ③—江南中生代隐伏断裂带; ④—政和-大埔断裂带; ⑤—鄰庐断裂带; ⑥—赣江断裂带;
- ⑦—马江断裂带; 深断裂带及编号: (1)吴川-四会; (2)抚州-遂川; (3)烟筒岭-南城; (4)政和-大埔; (5)汕头-安仁; (6)河源-邵武;
- (7)恩平-新丰-鹰潭; (8)东山-上杭

古元古代岩块、中元古代沉积岩、新元古代岩浆岩、泥砂质碎屑岩夹火山岩及碳酸盐岩 (Xia et al., 2012; Yu et al., 2012)。华南陆块的地质演化过程可概括为 4 个主要阶段: 太古宙—中元古代, 扬子地块和华夏地块分别在 3.8 Ga 和 1.9~1.8 Ga 形成了古老的结晶基底 (Jiao et al., 2009; Yu et al., 2010); 中元古代—新元古代 1.1~0.9 Ga, 扬子地块和华夏地块在江山-绍兴缝合带发生碰撞拼合, 形成了统一的华南陆块, 其拼合处形成了江南新元古代造山带 (Xu et al., 2012); 新元古代晚期约 8.25 Ga, 华南陆块发生裂解, 形成南华裂谷盆地 (Wang and Li, 2003; Li et al., 2005), 华夏地块裂解为武夷、云开和赣中南 3 个次级块体, 其间裂谷和深海槽堆积了早震旦世—晚奥陶世碎屑岩 (舒良树, 2012); 在早古生代的加里东期造山旋回中, 华南陆块沿江绍断裂带发生陆内俯冲, 导致南华裂谷闭合 (Charvet et al., 2010), 志留系沉积缺失, 上泥盆统砾岩以角度不整合覆盖在前泥盆系之上, 同时前泥盆系发生强烈变形, 并伴随大规模岩浆侵入, 形成了加里东期褶皱造山带 (Li et al., 2010b; Wang et al., 2011)。

2 样品采集与分析方法

研究区 9 件样品采自南迳盆地南部紧邻省道 346 线。岩石风化表面呈褐红色, 新鲜岩石呈浅灰色、灰绿色。挑选新鲜的变玄武岩样品磨成电子

探针片, 并进行背散射图像观察及电子探针成分分析。矿物的背散射图像观察及成分分析主要由东华理工大学核资源与环境国家重点实验室的 JEOL-JXA8530FPlus 型电子探针完成。测试条件为加速电压 15 kV, 电流 20 nA, 根据辉石颗粒的粒度大小、分布特征, 结合分析目标对精度的要求, 同时考虑仪器分辨率、检测时长等条件限制, 综合判断选择点分析或对辉石进行面扫。颗粒大者束斑直径选择 2 μm 。Si、Mg、Fe、Al、Ca、Na、K、F、Cl 等主量元素或易挥发元素特征峰测量时间为 10 s, 背景测量时间为 5 s; P、Ti、Cr、Ni、Mn 等微量元素特征峰测量时间为 20 s, 背景测量时间为 10 s, 所有测试数据均采用 ZAF 程序进行了校正处理。

主量、微量及稀土元素测试在科荟测试(天津)科技有限公司实验室完成, 样品由人工破碎至 200 目。主量元素采用 X 射线荧光法(XRF)在 XRF-1800X 荧光光谱仪上进行, 精度优于 2%; 微量元素及稀土元素利用高分辨电感耦合等离子体质谱仪(ICP-MS)在等离子质谱仪 Thermo Fisher Element XR 上测试完成, 精度优于 5%。

3 测试结果

3.1 岩相学特征

手标本样品颜色为灰绿色、浅灰绿色(图 2-a, b)。镜下观察变玄武岩呈变余粒状—柱状变晶结

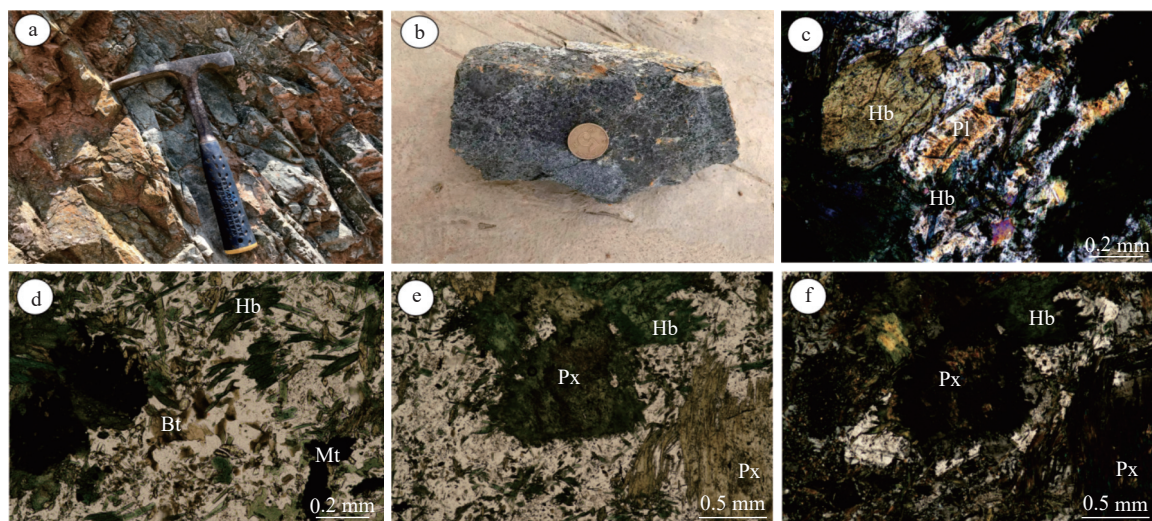


图 2 上洞变玄武岩手标本及岩相学照片

Fig. 2 Hand specimens and photomicrographs of the meta-basalt in Shangdong

a, b—变玄武岩手标本照片; c~f—变玄武岩镜下照片(c 和 f 为正交偏光; d 和 e 为单偏光)。

Hb—角闪石; Px—辉石; Pl—斜长石; Bt—黑云母; Mt—磁铁矿

构、变余斑状结构(图2-c, d),块状构造,斑晶为普通辉石、斜长石和角闪石,且多已破碎肢解,弱变形域可见少量残余的完整辉石(图2-e, f)。基质为角闪石、辉石和石英颗粒。组成矿物主要由角闪石(55%~75%)、斜长石(25%~40%)、辉石(10%~15%)、黑云母(10%~15%)组成,含有少量石英(1%~5%)。主要副矿物有磁铁矿。偶见角闪石双晶。角闪石常见有阳起石化、绿泥石化等。斜长石呈半自形板状结构,环带不明显,大多呈放射状排列,聚片双晶清晰。黑云母多呈半自形—他形,形态以片状为主,褐色—褐黄色多色性明显(图2-d)。基质为角闪石、辉石和石英颗粒。斑晶为普通辉石、斜长石和角闪石,斑晶多已破碎肢解,弱变形域内可见少量残余的完整辉石,残余辉石的形态表现为被局部包裹,岩石在形成后经历了特定的变质作用,使其矿物组合发生了显著变化,原始玄武岩的矿物组合转变为富含角闪石且局部保留辉石的新矿物组合,定名为变玄武岩(图2-e, f)。

3.2 矿物学特征

3.2.1 辉石

变玄武岩样品中辉石电子探针分析结果见表1。辉石是变玄武岩斑晶和基质的主要成分。辉石的背散射图像(BSE)及元素面扫描图(图3)显示,角闪石中残留辉石,表明部分角闪石是由辉石通过蚀变形成的。这一矿物转变过程反映原岩(玄武岩)在含流体条件下经历了变质作用,因而定名为变玄武岩,暗示其可能形成于热液蚀变、俯冲带或区域变质环境,记录了岩石受流体活动和温压条件影响的演化历史。辉石斑晶为富钙富镁富铁的普通辉石($Wo_{27\sim31}En_{40\sim48}Fs_{23\sim30}$;图4-a;表1)。Si和Al可以作为确定母岩浆类型的标型元素(孙传敏,1994)。辉石Si-Al^{IV}图(图4-b)显示,大部分单斜辉石落入拉斑玄武岩区。

3.2.2 黑云母

变玄武岩中黑云母的电子探针分析结果见表2。黑云母中氧化物总含量为93.14%~95.28%,处于含水矿物黑云母电子探针数据的允许误差内。黑云母表现为富铝、富铁、低镁、低钾的特征,为铁质黑云母(图5-a, a.p.f.u表示每分子式单位的原子数),黑云母 $Fe^{2+}/(Fe^{2+}+Mg)$ 值为0.49~0.53(平均值为0.51),变化范围均较小,显示黑云母未遭受后期流体作用的改造(Stone, 2000),指示其为岩浆成因。在

黑云母 $10TiO_2-TFeO-MgO$ 图解(图5-b)中,投点全部落在岩浆黑云母范围。

3.2.3 角闪石

选择原生角闪石进行电子探针测试分析,分析结果见表3。角闪石中 SiO_2 含量为41.17%~45.61%, $TFeO$ 含量为17.93%~21.94%, CaO 含量为11.49%~12.56%, MgO 含量为6.68%~10.20%, Al_2O_3 含量为9.70%~13.86%, TiO_2 含量为0.27%~0.48%, Na_2O 含量为0.70%~1.25%, K_2O 含量为0.21%~0.57%, MnO 含量为0.24%~0.35%。上洞变玄武岩中角闪石化学特征表现为富钙贫钛的特征,为钙质闪石组中的普通角闪石(图6), CaO 含量均大于11%,分子式中的Ti均小于0.06。

3.2.4 斜长石

斜长石是研究区变玄武岩的主要矿物,不仅是斑晶的主要成分,也是基质的主要矿物。斑晶中的斜长石呈长柱状,通常发育聚片双晶和简单双晶。斜长石为中长石-更长石($An_{16\sim44}Ab_{56\sim84}$;图7;表4)。斜长石中 TiO_2 含量低于0.15%,表明其可能经历了后期蚀变作用(Kerr, 1998)。变玄武岩普遍具变余斑状结构,基质矿物粒度细,暗色矿物含量高,推测原岩为玄武岩,可见斑晶主要为单斜辉石和斜长石,未见橄榄石斑晶。

3.3 岩石地球化学特征

3.3.1 主量元素

上洞变玄武岩主量元素分析结果见表5。全岩 SiO_2 含量在47.45%~49.49%之间,均落于基性岩浆岩区; Na_2O 含量为2.23%~3.03%, K_2O 含量为0.20%~0.43%,全碱(Na_2O+K_2O)含量介于2.50%~3.39%之间,表现出低碱的特点; K_2O/Na_2O 值介于0.07~0.16之间,均为 $Na_2O>K_2O$,岩石具明显的富钠贫钾特征; MgO 含量中等($MgO=5.53\% \sim 6.33\%$, $Mg^{\#}=40.44\sim45.16$)。 TFe_2O_3 为13.71%~14.95%, TiO_2 含量为2.14%~2.39%, Al_2O_3 介于14.05%~14.59%,总体显示低Ti、Al的特征。在火山岩 $Zr/TiO_2-Nb/Y$ 岩石化学分类图解(图8-a)上,样品点均落在亚碱性玄武岩区域。为了进一步确定样品的岩石类别,将样品投入玄武岩 $Zr-P_2O_5$ 判别图解(图8-b)中,样品点均落入到拉斑玄武岩系列。可见,上洞变玄武岩属于亚碱性拉斑玄武岩系列。

3.3.2 微量及稀土元素

上洞变玄武岩样品的微量和稀土元素分析测

表 1 辉石化学组成电子探针分析结果与结构计算

Table 1 Electron microporbe analyses and structural formula of pyroxene

%

续表1

| 样品号 | SD203-2 | | | | | | SD203-3 | | | | | | SD204-2 | | | | | | SD204-3 | | |
|--------------------------------|---------|-------|-------|-------|-------|-------|---------|-------|-------|-------|-------|-------|---------|-------|-------|-------|-------|-------|---------|-------|---|
| | 点号 | 14 | 15 | 3 | 9 | 10 | 13 | 15 | 17 | 2 | 3 | 4 | 5 | 7 | 8 | 9 | 10 | 13 | 1 | 2 | 3 |
| SiO ₂ | 52.32 | 52.19 | 51.09 | 51.63 | 51.08 | 52.36 | 50.87 | 52.49 | 52.90 | 52.37 | 52.46 | 53.18 | 52.85 | 52.35 | 52.73 | 53.55 | 51.79 | 50.74 | 52.69 | 50.71 | |
| Al ₂ O ₃ | 2.89 | 3.05 | 4.15 | 3.54 | 4.34 | 3.13 | 3.65 | 2.69 | 1.80 | 2.56 | 2.24 | 1.96 | 2.06 | 2.25 | 2.19 | 2.95 | 2.95 | 3.72 | 2.42 | 3.84 | |
| K ₂ O | 0.08 | 0.10 | 0.11 | 0.09 | 0.11 | 0.09 | 0.10 | 0.07 | 0.03 | 0.03 | 0.04 | 0.04 | 0.03 | 0.02 | 0.02 | 0.03 | 0.05 | 0.10 | 0.03 | 0.07 | |
| MnO | 0.32 | 0.30 | 0.28 | 0.32 | 0.33 | 0.28 | 0.35 | 0.30 | 0.30 | 0.30 | 0.22 | 0.24 | 0.30 | 0.29 | 0.29 | 0.28 | 0.27 | 0.27 | 0.28 | 0.30 | |
| TiO ₂ | 0.08 | 0.07 | 0.16 | 0.08 | 0.15 | 0.08 | 0.09 | 0.03 | 0.14 | 0.18 | 0.31 | 0.12 | 0.35 | 0.31 | 0.25 | 0.21 | 0.17 | 0.16 | 0.49 | 0.21 | |
| CaO | 12.14 | 12.18 | 13.03 | 13.17 | 13.11 | 12.22 | 12.11 | 12.29 | 12.25 | 12.15 | 12.25 | 12.25 | 12.25 | 12.24 | 12.25 | 11.47 | 12.33 | 12.19 | 12.46 | 12.09 | |
| Na ₂ O | 0.25 | 0.27 | 0.35 | 0.28 | 0.37 | 0.27 | 0.34 | 0.19 | 0.16 | 0.26 | 0.18 | 0.15 | 0.17 | 0.16 | 0.17 | 0.26 | 0.28 | 0.39 | 0.18 | 0.37 | |
| MgO | 13.23 | 13.38 | 13.62 | 14.49 | 13.70 | 13.51 | 13.07 | 12.99 | 14.68 | 14.04 | 14.31 | 14.42 | 14.34 | 14.30 | 14.42 | 13.25 | 14.51 | 12.84 | 14.88 | 13.23 | |
| Cl | 0.00 | 0.00 | 0.01 | 0.01 | 0.00 | 0.00 | 0.00 | 0.01 | 0.00 | 0.00 | 0.00 | 0.00 | 0.00 | 0.00 | 0.00 | 0.01 | 0.00 | 0.00 | 0.00 | 0.00 | |
| FeO | 15.76 | 15.26 | 15.52 | 15.01 | 15.69 | 14.93 | 15.44 | 16.10 | 14.11 | 14.38 | 14.58 | 14.26 | 14.20 | 14.41 | 14.41 | 15.07 | 13.96 | 16.21 | 14.15 | 15.76 | |
| P ₂ O ₅ | 0.00 | 0.04 | 0.03 | 0.00 | 0.01 | 0.01 | 0.00 | 0.00 | 0.02 | 0.00 | 0.02 | 0.03 | 0.00 | 0.01 | 0.02 | 0.01 | 0.00 | 0.00 | 0.00 | 0.01 | |
| 总计 | 97.08 | 96.84 | 98.35 | 98.62 | 98.91 | 96.91 | 96.27 | 97.18 | 96.40 | 96.31 | 96.62 | 96.66 | 96.56 | 96.43 | 96.80 | 97.09 | 96.45 | 96.68 | 97.65 | 96.63 | |
| Ca | 0.51 | 0.51 | 0.53 | 0.54 | 0.54 | 0.51 | 0.51 | 0.51 | 0.51 | 0.51 | 0.51 | 0.51 | 0.51 | 0.51 | 0.51 | 0.48 | 0.51 | 0.51 | 0.51 | 0.51 | |
| Mg | 0.77 | 0.78 | 0.78 | 0.82 | 0.78 | 0.78 | 0.78 | 0.77 | 0.85 | 0.82 | 0.83 | 0.84 | 0.83 | 0.83 | 0.84 | 0.77 | 0.84 | 0.75 | 0.85 | 0.77 | |
| Ti | 0.00 | 0.00 | 0.00 | 0.00 | 0.00 | 0.00 | 0.00 | 0.00 | 0.00 | 0.01 | 0.01 | 0.00 | 0.01 | 0.01 | 0.01 | 0.01 | 0.01 | 0.00 | 0.01 | 0.01 | |
| Si | 2.04 | 2.04 | 1.96 | 1.97 | 1.95 | 2.04 | 2.04 | 2.00 | 2.06 | 2.05 | 2.05 | 2.07 | 2.06 | 2.05 | 2.05 | 2.09 | 2.02 | 1.99 | 2.03 | 1.98 | |
| Al ^{IV} | 0.13 | 0.14 | 0.17 | 0.16 | 0.17 | 0.14 | 0.14 | 0.17 | 0.08 | 0.12 | 0.10 | 0.09 | 0.09 | 0.10 | 0.10 | 0.14 | 0.14 | 0.17 | 0.11 | 0.16 | |
| Al ^{VI} | 0.00 | 0.00 | 0.02 | 0.00 | 0.02 | 0.00 | 0.00 | 0.00 | 0.00 | 0.00 | 0.00 | 0.00 | 0.00 | 0.00 | 0.00 | 0.00 | 0.00 | 0.00 | 0.00 | 0.01 | |
| Fe ³⁺ | 0.00 | 0.00 | 0.00 | 0.00 | 0.00 | 0.00 | 0.00 | 0.00 | 0.00 | 0.00 | 0.00 | 0.00 | 0.00 | 0.00 | 0.00 | 0.00 | 0.00 | 0.00 | 0.00 | 0.00 | |
| Fe ²⁺ | 0.51 | 0.49 | 0.49 | 0.48 | 0.50 | 0.48 | 0.48 | 0.50 | 0.45 | 0.46 | 0.47 | 0.46 | 0.45 | 0.46 | 0.46 | 0.48 | 0.45 | 0.53 | 0.45 | 0.51 | |
| Mn | 0.01 | 0.01 | 0.01 | 0.01 | 0.01 | 0.01 | 0.01 | 0.01 | 0.01 | 0.01 | 0.01 | 0.01 | 0.01 | 0.01 | 0.01 | 0.01 | 0.01 | 0.01 | 0.01 | 0.01 | |
| K | 0.00 | 0.01 | 0.01 | 0.00 | 0.01 | 0.00 | 0.00 | 0.01 | 0.00 | 0.00 | 0.00 | 0.00 | 0.00 | 0.00 | 0.00 | 0.00 | 0.00 | 0.01 | 0.00 | 0.00 | |
| P | 0.00 | 0.00 | 0.00 | 0.00 | 0.00 | 0.00 | 0.00 | 0.00 | 0.00 | 0.00 | 0.00 | 0.00 | 0.00 | 0.00 | 0.00 | 0.00 | 0.00 | 0.00 | 0.00 | 0.00 | |
| Na | 0.02 | 0.02 | 0.03 | 0.02 | 0.03 | 0.02 | 0.02 | 0.03 | 0.01 | 0.02 | 0.01 | 0.01 | 0.01 | 0.01 | 0.01 | 0.02 | 0.02 | 0.03 | 0.01 | 0.03 | |
| 总计 | 3.99 | 3.99 | 4.00 | 4.00 | 3.99 | 3.99 | 3.99 | 3.99 | 3.99 | 3.99 | 3.99 | 3.99 | 3.99 | 3.99 | 3.99 | 3.99 | 3.99 | 3.99 | 3.99 | 3.99 | |
| En | 42.46 | 43.06 | 42.24 | 44.08 | 42.09 | 43.53 | 43.53 | 42.19 | 46.37 | 44.97 | 45.40 | 45.91 | 45.73 | 45.51 | 45.68 | 43.82 | 45.90 | 41.06 | 46.42 | 42.23 | |
| Fs | 28.49 | 27.66 | 27.32 | 26.01 | 27.48 | 27.04 | 27.04 | 28.29 | 25.13 | 25.97 | 25.93 | 25.44 | 25.48 | 25.82 | 25.71 | 27.79 | 24.94 | 29.28 | 24.90 | 28.49 | |
| Wo | 28.00 | 28.17 | 29.05 | 28.80 | 28.96 | 28.30 | 28.30 | 28.10 | 27.82 | 27.97 | 27.92 | 28.04 | 28.09 | 28.00 | 27.90 | 27.26 | 28.03 | 28.02 | 27.94 | 27.75 | |
| Mg [#] | 0.53 | 0.54 | 0.57 | 0.61 | 0.58 | 0.53 | 0.54 | 0.54 | 0.56 | 0.55 | 0.55 | 0.55 | 0.55 | 0.55 | 0.49 | 0.58 | 0.54 | 0.57 | 0.55 | | |
| Fe* | 0.53 | 0.51 | 0.50 | 0.49 | 0.51 | 0.50 | 0.52 | 0.54 | 0.47 | 0.48 | 0.48 | 0.47 | 0.47 | 0.48 | 0.48 | 0.50 | 0.46 | 0.54 | 0.47 | 0.53 | |
| 属性 | 普通辉石 | | | | | | | | | | | | | | | | | | | | |

注:以6个O原子为基准计算的阳离子

试结果及相关数据见表6。稀土元素总量较低($75.61 \times 10^{-6} \sim 102.17 \times 10^{-6}$),表现为轻、重稀土元素中—弱分异($\text{La/Yb}_N=2.48 \sim 2.81$; LREE/HREE值为 $3.08 \sim 3.39$,平均值为3.30,富集轻稀土元素; $\delta\text{Eu}=1.03 \sim 1.11$,无显著Eu异常,呈右倾平坦型,类

似于E-MORB稀土元素配分模式(图9-b)。微量元素以弱亏损Sr-Nb-Ta和高的Nb/La、Nb/U值为特征(图9-a、图10),而高的Nb含量($9.51 \times 10^{-6} \sim 12.88 \times 10^{-6}$)和高的Nb/La($0.97 \sim 1.02$)、Nb/U($28.25 \sim 32.79$),与富Nb玄武岩类似(NEBA,图10)。

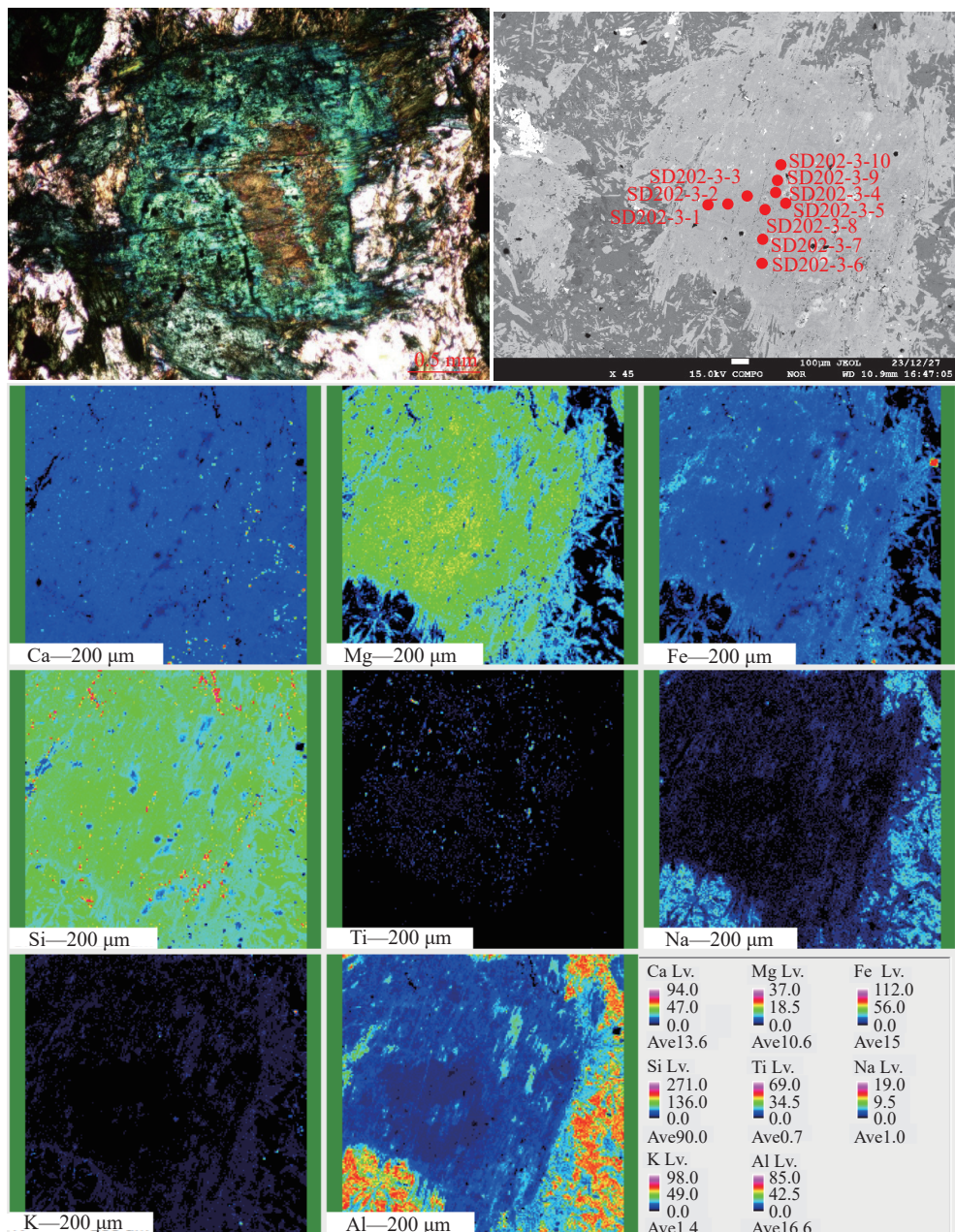


图3 辉石正交偏光、背散射 (BSE) 图像和对应 Ca、Mg、Fe、Si、Ti、Na、K、Al 元素面扫描图(单位为质量分数 %)

Fig. 3 Orthogonal polarization image, Backscattered Electron (BSE) image and corresponding elemental mapping of Ca, Mg, Fe, Si, Ti, Na, K, Al in pyroxene

$^{143}\text{Nd}/^{144}\text{Nd}$ 值变化于 0.512860~0.512862 之间, 对应的 $\varepsilon_{\text{Nd}}(t)$ 值介于 6.15~6.38 之间。

4 讨论

4.1 成岩物理化学条件

单斜辉石、角闪石、黑云母等暗色矿物的化学组成与形成环境有关, 其化学特征除反映岩石成因类型和构造环境外, 还能反映岩浆冷凝结晶时的压力、

温度、氧逸度等成岩条件 (姜常义和安三元, 1984; 周作侠, 1988; 牛漫兰等, 2018)。本次选择变玄武岩中的辉石、角闪石、黑云母为对象, 开展成岩物理化学条件研究。

Thompson(1974) 建立了以单斜辉石中 Al 含量为参数, 计算不同类型玄武岩中单斜辉石结晶温度和压力的公式。周新民等 (1982) 在此基础上总结了碱性玄武岩中单斜辉石的温压回归方程:

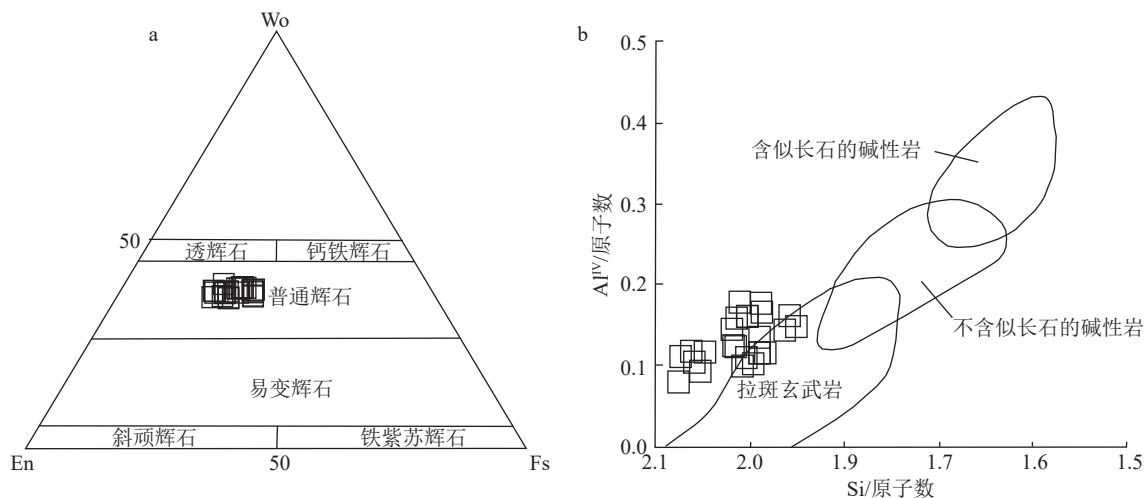
图4 辉石 Wo-En-Fs 分类图解 (a, 据 Morimoto, 1988) 和 Si-Al^{IV} 图 (b, 据 Kushiro, 1960)Fig. 4 Wo-En-Fs diagram of clinopyroxenes (a) and Si-Al^{IV} diagram of pyroxene (b)

表2 黑云母电子探针分析结果

Table 2 Electron microprobe analyses of biotite

%

| 样品号 | SD204-1 | | | | | | | | | | SD204-2 | | | | |
|--------------------------------|---------|-------|-------|-------|-------|-------|-------|-------|-------|-------|---------|-------|-------|-------|-------|
| | 6 | 8 | 11 | 12 | 14 | 15 | 16 | 19 | 20 | 22 | 19 | 20 | 21 | 23 | 24 |
| SiO ₂ | 35.52 | 36.13 | 35.28 | 35.44 | 35.79 | 35.15 | 34.84 | 35.39 | 35.65 | 35.48 | 35.39 | 35.63 | 34.99 | 35.57 | 35.51 |
| Al ₂ O ₃ | 16.06 | 15.47 | 15.41 | 13.98 | 16.04 | 15.34 | 15.62 | 15.72 | 15.14 | 15.81 | 16.28 | 15.74 | 15.77 | 15.95 | 16.22 |
| K ₂ O | 9.36 | 9.25 | 9.33 | 9.35 | 9.41 | 9.23 | 8.99 | 9.13 | 9.20 | 9.01 | 9.40 | 9.38 | 9.19 | 9.27 | 8.63 |
| MnO | 0.15 | 0.11 | 0.13 | 0.16 | 0.17 | 0.15 | 0.13 | 0.11 | 0.12 | 0.15 | 0.20 | 0.17 | 0.15 | 0.17 | 0.14 |
| Cr ₂ O ₃ | 0.04 | 0.07 | 0.08 | 0.12 | 0.03 | 0.24 | 0.99 | 0.09 | 0.03 | 0.10 | 0.02 | 0.04 | 0.12 | 0.02 | 0.10 |
| TiO ₂ | 2.81 | 3.06 | 2.60 | 2.64 | 2.68 | 2.75 | 2.80 | 2.87 | 2.93 | 2.82 | 2.55 | 2.58 | 2.70 | 2.45 | 2.31 |
| CaO | 0.00 | 0.05 | 0.04 | 0.02 | 0.02 | 0.05 | 0.09 | 0.05 | 0.03 | 0.07 | 0.11 | 0.08 | 0.13 | 0.08 | 0.18 |
| NiO | 0.00 | 0.00 | 0.00 | 0.02 | 0.00 | 0.01 | 0.00 | 0.02 | 0.03 | 0.02 | 0.03 | 0.00 | 0.02 | 0.00 | 0.03 |
| Na ₂ O | 0.02 | 0.03 | 0.06 | 0.07 | 0.04 | 0.03 | 0.02 | 0.05 | 0.04 | 0.06 | 0.11 | 0.05 | 0.11 | 0.05 | 0.06 |
| MgO | 9.41 | 9.74 | 9.68 | 10.04 | 9.74 | 9.87 | 9.79 | 9.58 | 9.72 | 9.66 | 9.39 | 9.55 | 9.54 | 9.75 | 9.88 |
| F | 0.00 | 0.00 | 0.00 | 0.00 | 0.00 | 0.00 | 0.00 | 0.00 | 0.46 | 0.63 | 0.85 | 0.00 | 0.00 | 0.00 | 0.00 |
| Cl | 0.02 | 0.00 | 0.01 | 0.02 | 0.01 | 0.01 | 0.01 | 0.02 | 0.01 | 0.01 | 0.01 | 0.00 | 0.01 | 0.01 | 0.02 |
| TFeO | 21.44 | 21.19 | 21.21 | 21.28 | 21.34 | 20.81 | 20.75 | 21.04 | 21.01 | 20.88 | 20.70 | 21.15 | 20.72 | 20.73 | 20.60 |
| P ₂ O ₅ | 0.00 | 0.00 | 0.00 | 0.00 | 0.01 | 0.01 | 0.00 | 0.00 | 0.02 | 0.01 | 0.00 | 0.00 | 0.00 | 0.00 | 0.01 |
| 总计 | 94.83 | 95.10 | 93.83 | 93.14 | 95.28 | 93.63 | 94.03 | 94.05 | 94.39 | 94.71 | 95.04 | 94.36 | 93.46 | 94.06 | 93.69 |
| Si | 5.51 | 5.61 | 5.48 | 5.50 | 5.55 | 5.45 | 5.41 | 5.49 | 5.53 | 5.51 | 5.49 | 5.53 | 5.43 | 5.52 | 5.51 |
| Al ^{IV} | 2.49 | 2.39 | 2.52 | 2.50 | 2.45 | 2.55 | 2.59 | 2.51 | 2.47 | 2.49 | 2.51 | 2.47 | 2.57 | 2.48 | 2.49 |
| Al ^{VI} | 0.45 | 0.44 | 0.29 | 0.06 | 0.49 | 0.26 | 0.27 | 0.37 | 0.30 | 0.40 | 0.47 | 0.41 | 0.32 | 0.44 | 0.48 |
| Ti | 0.33 | 0.36 | 0.30 | 0.31 | 0.31 | 0.32 | 0.33 | 0.34 | 0.34 | 0.33 | 0.30 | 0.30 | 0.31 | 0.29 | 0.27 |
| Fe ³⁺ | 0.41 | 0.24 | 0.24 | 0.41 | 0.42 | 0.41 | 0.42 | 0.23 | 0.48 | 0.48 | 0.50 | 0.42 | 0.40 | 0.40 | 0.38 |
| Fe ²⁺ | 2.34 | 2.48 | 2.56 | 2.32 | 2.26 | 2.34 | 2.32 | 2.47 | 2.24 | 2.19 | 2.23 | 2.25 | 2.31 | 2.28 | 2.36 |
| Mn | 0.02 | 0.01 | 0.02 | 0.02 | 0.02 | 0.02 | 0.02 | 0.01 | 0.02 | 0.02 | 0.03 | 0.02 | 0.02 | 0.02 | 0.02 |
| Mg | 2.18 | 2.25 | 2.24 | 2.32 | 2.25 | 2.28 | 2.26 | 2.22 | 2.25 | 2.24 | 2.17 | 2.21 | 2.21 | 2.26 | 2.29 |
| Ca | 0.00 | 0.01 | 0.01 | 0.00 | 0.00 | 0.01 | 0.02 | 0.01 | 0.00 | 0.01 | 0.02 | 0.01 | 0.02 | 0.01 | 0.03 |
| Na | 0.01 | 0.01 | 0.02 | 0.02 | 0.01 | 0.01 | 0.01 | 0.01 | 0.02 | 0.03 | 0.01 | 0.03 | 0.02 | 0.02 | 0.02 |
| K | 1.85 | 1.83 | 1.85 | 1.85 | 1.86 | 1.83 | 1.78 | 1.81 | 1.82 | 1.78 | 1.86 | 1.86 | 1.82 | 1.83 | 1.71 |
| Cl | 0.00 | 0.00 | 0.00 | 0.00 | 0.00 | 0.00 | 0.00 | 0.01 | 0.00 | 0.00 | 0.00 | 0.00 | 0.00 | 0.00 | 0.00 |
| F | 0.00 | 0.00 | 0.00 | 0.00 | 0.00 | 0.00 | 0.00 | 0.00 | 0.23 | 0.31 | 0.42 | 0.00 | 0.00 | 0.00 | 0.00 |
| 总计 | 15.59 | 15.63 | 15.53 | 15.32 | 15.64 | 15.48 | 15.42 | 15.47 | 15.70 | 15.78 | 16.03 | 15.50 | 15.45 | 15.55 | 15.55 |
| Mg [#] | 0.44 | 0.45 | 0.45 | 0.46 | 0.45 | 0.46 | 0.46 | 0.45 | 0.45 | 0.45 | 0.45 | 0.45 | 0.46 | 0.46 | 0.46 |

注:以22个氧原子为基准计算的阳离子

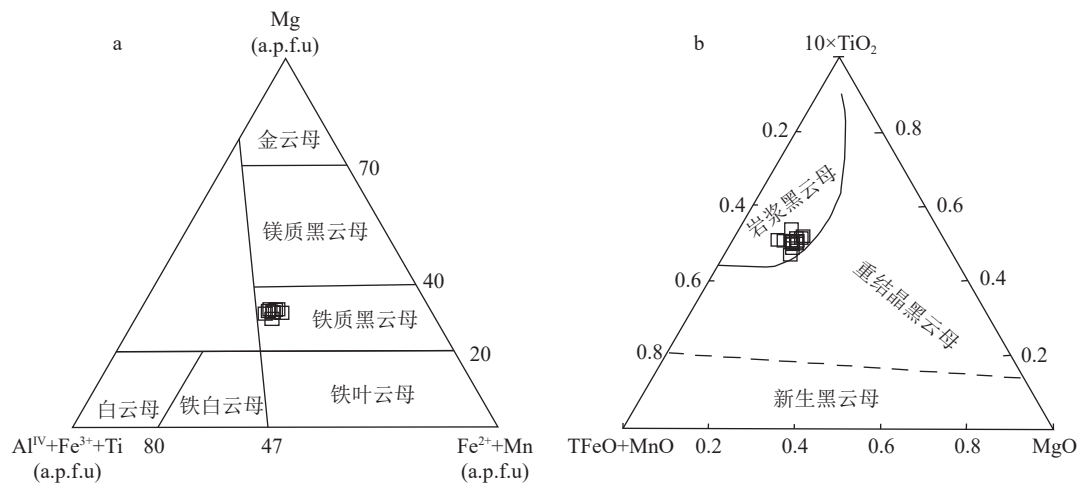
图5 黑云母分类图解(a, 据 Foster, 1960) 和黑云母成分 10×TiO₂-TFeO-MgO 图解(b, 据 Nachit et al., 2005)Fig. 5 Biotite classification diagram (a) and 10×TiO₂-TFeO-MgO diagram of biotite (b)

表3 角闪石电子探针分析数据

Table 3 Electron microprobe analyses of amphibol

%

| 样品号 | SD202-1 | | | | | | | | | | | | | | | | | | | | SD203-2 | | | | | | | | | | | | | |
|--------------------------------|---------|-------|-------|-------|-------|-------|-------|-------|-------|-------|-------|-------|-------|-------|-------|-------|-------|-------|-------|-------|---------|-------|-------|-------|--|--|--|--|--|--|--|--|--|--|
| | 6 | 7 | 8 | 9 | 10 | 16 | 17 | 18 | 19 | 20 | 21 | 22 | 23 | 24 | 25 | 36 | 37 | 38 | 39 | 40 | 41 | 42 | 43 | 44 | | | | | | | | | | |
| SiO ₂ | 43.44 | 43.33 | 44.64 | 44.56 | 45.61 | 43.59 | 43.79 | 44.99 | 44.22 | 43.12 | 44.98 | 43.64 | 43.36 | 44.80 | 44.57 | 41.17 | 42.01 | 42.20 | 42.07 | 41.36 | 41.54 | 41.53 | 42.53 | 43.95 | | | | | | | | | | |
| Al ₂ O ₃ | 11.65 | 11.70 | 11.04 | 11.09 | 9.70 | 11.12 | 11.12 | 9.95 | 10.78 | 11.76 | 10.57 | 11.70 | 11.71 | 9.82 | 10.47 | 13.86 | 12.56 | 12.21 | 12.71 | 12.14 | 12.71 | 13.17 | 12.36 | 11.31 | | | | | | | | | | |
| K ₂ O | 0.31 | 0.38 | 0.29 | 0.23 | 0.29 | 0.37 | 0.34 | 0.29 | 0.23 | 0.37 | 0.22 | 0.26 | 0.33 | 0.21 | 0.30 | 0.49 | 0.57 | 0.35 | 0.35 | 0.51 | 0.57 | 0.53 | 0.41 | 0.43 | | | | | | | | | | |
| MnO | 0.29 | 0.28 | 0.24 | 0.26 | 0.25 | 0.24 | 0.27 | 0.29 | 0.30 | 0.27 | 0.31 | 0.33 | 0.32 | 0.34 | 0.26 | 0.34 | 0.26 | 0.33 | 0.29 | 0.30 | 0.27 | 0.25 | 0.30 | 0.35 | | | | | | | | | | |
| TiO ₂ | 0.32 | 0.34 | 0.28 | 0.30 | 0.34 | 0.37 | 0.27 | 0.27 | 0.33 | 0.34 | 0.33 | 0.41 | 0.41 | 0.36 | 0.35 | 0.35 | 0.42 | 0.34 | 0.38 | 0.48 | 0.47 | 0.36 | 0.37 | 0.33 | | | | | | | | | | |
| CaO | 12.78 | 12.79 | 12.82 | 12.73 | 12.80 | 12.72 | 12.21 | 12.66 | 12.66 | 12.68 | 12.89 | 12.61 | 12.62 | 12.73 | 12.91 | 11.76 | 11.64 | 11.49 | 11.87 | 11.67 | 11.79 | 11.75 | 11.71 | 11.81 | | | | | | | | | | |
| Na ₂ O | 0.96 | 0.94 | 0.93 | 0.85 | 0.70 | 0.89 | 0.77 | 0.85 | 0.90 | 0.99 | 0.73 | 0.86 | 0.93 | 0.85 | 0.85 | 1.25 | 1.06 | 1.15 | 1.14 | 1.11 | 1.08 | 1.09 | 1.07 | 0.95 | | | | | | | | | | |
| MgO | 8.78 | 8.72 | 9.07 | 9.31 | 10.20 | 8.51 | 9.31 | 9.80 | 9.33 | 8.90 | 9.48 | 8.79 | 8.66 | 9.82 | 9.40 | 6.68 | 7.28 | 7.34 | 7.38 | 7.52 | 7.12 | 7.05 | 7.40 | 8.25 | | | | | | | | | | |
| TFeO | 19.15 | 19.19 | 18.07 | 18.54 | 17.93 | 19.44 | 18.46 | 18.34 | 18.90 | 19.04 | 18.21 | 18.80 | 19.13 | 18.17 | 18.78 | 20.05 | 19.28 | 19.35 | 19.79 | 19.97 | 21.94 | 21.68 | 21.19 | 20.13 | | | | | | | | | | |
| 总计 | 97.67 | 97.68 | 97.39 | 97.88 | 97.81 | 97.25 | 96.53 | 97.43 | 97.65 | 97.47 | 97.73 | 97.39 | 97.47 | 97.09 | 97.89 | 95.95 | 95.07 | 94.78 | 95.96 | 95.07 | 97.49 | 97.41 | 97.35 | 97.50 | | | | | | | | | | |
| Mn | 0.04 | 0.04 | 0.03 | 0.03 | 0.03 | 0.03 | 0.04 | 0.04 | 0.03 | 0.04 | 0.04 | 0.04 | 0.04 | 0.04 | 0.03 | 0.04 | 0.03 | 0.04 | 0.04 | 0.04 | 0.03 | 0.03 | 0.04 | 0.04 | | | | | | | | | | |
| Na | 0.28 | 0.27 | 0.27 | 0.25 | 0.20 | 0.26 | 0.22 | 0.25 | 0.26 | 0.29 | 0.21 | 0.25 | 0.27 | 0.25 | 0.25 | 0.37 | 0.32 | 0.35 | 0.34 | 0.33 | 0.31 | 0.32 | 0.31 | 0.28 | | | | | | | | | | |
| Mg | 1.96 | 1.95 | 2.03 | 2.06 | 2.25 | 1.92 | 2.08 | 2.18 | 2.07 | 1.99 | 2.10 | 1.96 | 1.94 | 2.19 | 2.09 | 1.53 | 1.67 | 1.69 | 1.68 | 1.73 | 1.60 | 1.59 | 1.66 | 1.84 | | | | | | | | | | |
| K | 0.06 | 0.07 | 0.06 | 0.04 | 0.05 | 0.07 | 0.06 | 0.06 | 0.04 | 0.07 | 0.04 | 0.05 | 0.06 | 0.04 | 0.06 | 0.10 | 0.11 | 0.07 | 0.07 | 0.10 | 0.11 | 0.10 | 0.08 | 0.08 | | | | | | | | | | |
| Si | 6.51 | 6.50 | 6.69 | 6.62 | 6.76 | 6.58 | 6.57 | 6.71 | 6.60 | 6.47 | 6.70 | 6.53 | 6.51 | 6.71 | 6.65 | 6.31 | 6.48 | 6.51 | 6.43 | 6.39 | 6.27 | 6.26 | 6.40 | 6.57 | | | | | | | | | | |
| Al | 2.06 | 2.07 | 1.95 | 1.94 | 1.69 | 1.98 | 1.97 | 1.75 | 1.90 | 2.08 | 1.86 | 2.06 | 2.07 | 1.73 | 1.84 | 2.50 | 2.28 | 2.22 | 2.29 | 2.21 | 2.26 | 2.34 | 2.19 | 1.99 | | | | | | | | | | |
| Ca | 2.05 | 2.06 | 2.06 | 2.03 | 2.03 | 2.06 | 1.96 | 2.02 | 2.02 | 2.04 | 2.06 | 2.02 | 2.03 | 2.04 | 2.06 | 1.93 | 1.92 | 1.90 | 1.94 | 1.93 | 1.91 | 1.90 | 1.89 | 1.89 | | | | | | | | | | |
| Ti | 0.04 | 0.04 | 0.03 | 0.03 | 0.04 | 0.04 | 0.03 | 0.03 | 0.04 | 0.04 | 0.04 | 0.05 | 0.05 | 0.04 | 0.04 | 0.04 | 0.05 | 0.04 | 0.04 | 0.06 | 0.05 | 0.04 | 0.04 | 0.04 | | | | | | | | | | |
| Fe ³⁺ | 0.41 | 0.40 | 0.15 | 0.40 | 0.38 | 0.33 | 0.62 | 0.41 | 0.49 | 0.47 | 0.31 | 0.43 | 0.44 | 0.39 | 0.34 | 0.46 | 0.39 | 0.47 | 0.49 | 0.62 | 0.84 | 0.83 | 0.76 | 0.65 | | | | | | | | | | |
| Fe ²⁺ | 1.99 | 2.01 | 2.11 | 1.90 | 1.84 | 2.12 | 1.70 | 1.88 | 1.87 | 1.92 | 1.96 | 1.92 | 1.96 | 1.89 | 2.00 | 2.11 | 2.09 | 2.03 | 2.04 | 1.96 | 1.93 | 1.91 | 1.91 | 1.87 | | | | | | | | | | |
| Al ^{IV} | 1.49 | 1.50 | 1.31 | 1.38 | 1.24 | 1.42 | 1.43 | 1.29 | 1.40 | 1.53 | 1.30 | 1.47 | 1.49 | 1.29 | 1.35 | 1.69 | 1.52 | 1.49 | 1.57 | 1.61 | 1.73 | 1.74 | 1.60 | 1.43 | | | | | | | | | | |
| Al ^{VII} | 0.57 | 0.57 | 0.65 | 0.56 | 0.46 | 0.56 | 0.54 | 0.46 | 0.49 | 0.55 | 0.55 | 0.60 | 0.58 | 0.45 | 0.49 | 0.82 | 0.76 | 0.73 | 0.71 | 0.60 | 0.54 | 0.61 | 0.59 | 0.56 | | | | | | | | | | |
| Mg/(Mg+Fe) | 0.50 | 0.49 | 0.49 | 0.52 | 0.55 | 0.47 | 0.55 | 0.54 | 0.53 | 0.51 | 0.52 | 0.51 | 0.50 | 0.54 | 0.51 | 0.42 | 0.44 | 0.45 | 0.45 | 0.47 | 0.45 | 0.45 | 0.47 | 0.50 | | | | | | | | | | |
| T/°C | 572 | 585 | 551 | 562 | 582 | 605 | 544 | 542 | 577 | 583 | 579 | 625 | 624 | 594 | 588 | 593 | 634 | 593 | 609 | 675 | 662 | 600 | 601 | 577 | | | | | | | | | | |

注:以23个O原子为标准计算;钙质角闪石Ti温度计经验公式: $T(^\circ\text{C})=389+5098.36\text{Ti}(\text{Ti}<0.054)$

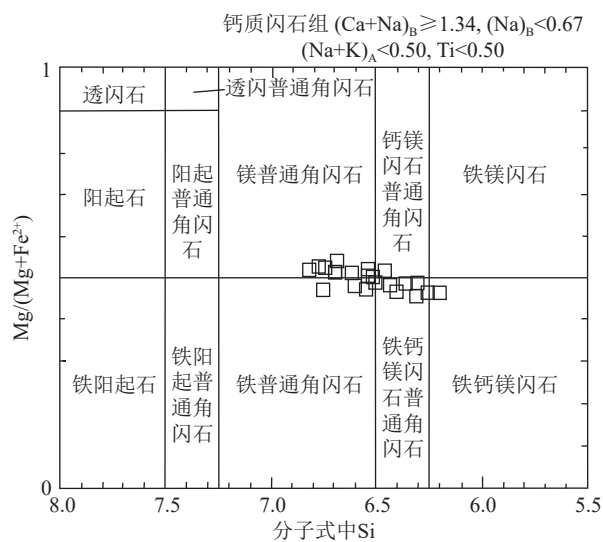


图6 角闪石分类及成因判别图解(据靳是琴, 1991)

Fig. 6 Classification and origin distinguishing of hornblende

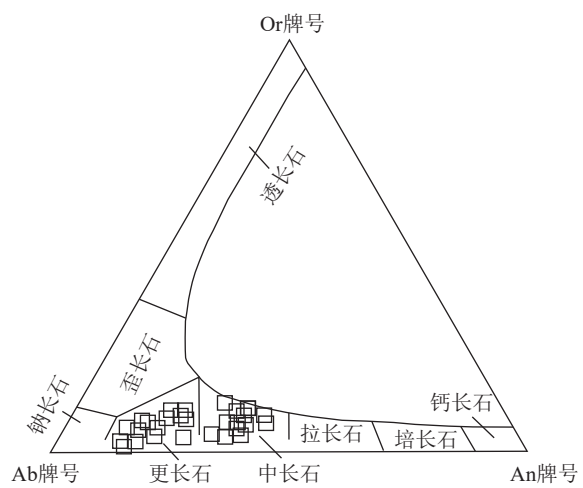


图7 斜长石成分分类图解(据Deer, 1992)

Fig. 7 Classification diagram of plagioclase

表4 斜长石化学组分电子探针分析结果

Table 4 EPMA results of the plagioclase chemical composition

%

| 样品号 | SD203-1 | | | | | SD203-2 | | | | | SD203-2 | | | | | | |
|--------------------------------|---------|-------|--------|-------|-------|---------|--------|--------|-------|-------|---------|--------|--------|--------|--------|--------|-------|
| | 26 | 28 | 29 | 30 | 1 | 2 | 3 | 4 | 5 | 7 | 8 | 9 | 10 | 11 | 12 | 13 | 14 |
| SiO ₂ | 60.26 | 63.95 | 67.59 | 61.37 | 58.89 | 60.56 | 59.16 | 58.74 | 58.74 | 60.21 | 61.98 | 58.55 | 64.04 | 63.82 | 63.81 | 59.31 | 58.38 |
| Al ₂ O ₃ | 25.54 | 23.05 | 21.44 | 24.51 | 26.38 | 25.77 | 27.02 | 26.72 | 26.39 | 25.28 | 25.92 | 26.81 | 22.89 | 24.14 | 23.84 | 26.37 | 26.41 |
| K ₂ O | 0.04 | 0.04 | 0.06 | 0.05 | 0.05 | 0.09 | 0.05 | 0.05 | 0.04 | 0.05 | 0.05 | 0.04 | 0.05 | 0.03 | 0.06 | 0.04 | 0.04 |
| MnO | 0.00 | 0.04 | 0.00 | 0.02 | 0.02 | 0.02 | 0.00 | 0.00 | 0.00 | 0.01 | 0.01 | 0.00 | 0.01 | 0.01 | 0.00 | 0.00 | 0.00 |
| TiO ₂ | 0.00 | 0.00 | 0.00 | 0.00 | 0.00 | 0.00 | 0.00 | 0.00 | 0.00 | 0.00 | 0.00 | 0.00 | 0.00 | 0.00 | 0.00 | 0.00 | 0.00 |
| CaO | 6.55 | 3.57 | 3.14 | 5.74 | 7.92 | 6.71 | 8.10 | 8.20 | 7.85 | 6.69 | 6.44 | 8.19 | 5.41 | 4.59 | 4.40 | 7.57 | 7.98 |
| Na ₂ O | 7.22 | 8.97 | 8.57 | 7.79 | 6.59 | 7.14 | 6.27 | 6.46 | 6.67 | 7.01 | 6.68 | 6.32 | 7.91 | 7.38 | 8.00 | 6.62 | 6.49 |
| MgO | 0.00 | 0.02 | 0.00 | 0.00 | 0.00 | 0.00 | 0.01 | 0.00 | 0.02 | 0.02 | 0.00 | 0.00 | 0.00 | 0.00 | 0.00 | 0.00 | 0.00 |
| TFeO | 0.04 | 0.04 | 0.09 | 0.20 | 0.11 | 0.04 | 0.08 | 0.09 | 0.07 | 0.04 | 0.16 | 0.15 | 0.10 | 0.07 | 0.06 | 0.23 | 0.17 |
| 总计 | 99.66 | 99.68 | 100.88 | 99.69 | 99.98 | 100.41 | 100.73 | 100.26 | 99.89 | 99.56 | 101.24 | 100.10 | 100.42 | 100.23 | 100.20 | 100.15 | 99.48 |
| Si | 10.73 | 11.39 | 12.04 | 10.93 | 10.49 | 10.79 | 10.54 | 10.46 | 10.46 | 10.69 | 11.01 | 10.40 | 11.37 | 11.33 | 11.33 | 10.53 | 10.37 |
| Al | 5.36 | 4.84 | 4.50 | 5.15 | 5.54 | 5.41 | 5.67 | 5.61 | 5.54 | 5.29 | 5.43 | 5.61 | 4.79 | 5.05 | 4.99 | 5.52 | 5.53 |
| Fe | 0.01 | 0.01 | 0.01 | 0.03 | 0.02 | 0.01 | 0.01 | 0.01 | 0.01 | 0.01 | 0.02 | 0.02 | 0.01 | 0.01 | 0.01 | 0.03 | 0.03 |
| Ca | 1.25 | 0.68 | 0.60 | 1.10 | 1.51 | 1.28 | 1.55 | 1.56 | 1.50 | 1.27 | 1.22 | 1.56 | 1.03 | 0.87 | 0.84 | 1.44 | 1.52 |
| Na | 2.49 | 3.10 | 2.96 | 2.69 | 2.27 | 2.46 | 2.16 | 2.23 | 2.30 | 2.41 | 2.30 | 2.17 | 2.72 | 2.54 | 2.76 | 2.28 | 2.24 |
| K | 0.01 | 0.01 | 0.01 | 0.01 | 0.01 | 0.02 | 0.01 | 0.01 | 0.01 | 0.01 | 0.01 | 0.01 | 0.01 | 0.01 | 0.01 | 0.01 | 0.01 |
| 总计 | 19.85 | 20.02 | 20.12 | 19.90 | 19.84 | 19.97 | 19.94 | 19.89 | 19.82 | 19.69 | 19.99 | 19.78 | 19.94 | 19.82 | 19.94 | 19.82 | 19.69 |
| An | 33.30 | 17.96 | 16.78 | 28.87 | 39.79 | 34.00 | 41.55 | 41.10 | 39.34 | 34.41 | 34.61 | 41.64 | 27.33 | 25.51 | 23.21 | 38.62 | 40.33 |
| Ab | 66.46 | 81.80 | 82.85 | 70.82 | 59.91 | 65.48 | 58.17 | 58.63 | 60.43 | 65.26 | 65.05 | 58.11 | 72.39 | 74.27 | 76.42 | 61.16 | 59.41 |
| Or | 0.24 | 0.24 | 0.38 | 0.31 | 0.29 | 0.52 | 0.28 | 0.27 | 0.23 | 0.33 | 0.33 | 0.25 | 0.28 | 0.23 | 0.38 | 0.22 | 0.26 |
| 端元 | 中长石 | 奥长石 | 奥长石 | 奥长石 | 中长石 | 中长石 | 中长石 | 中长石 | 中长石 | 中长石 | 中长石 | 奥长石 | 奥长石 | 奥长石 | 中长石 | 中长石 | |

续表4

| 样品号 | SD203-2 | | | | | | | | | | | | SD203-3 | | | | | | | | |
|--------------------------------|---------|--------|--------|--------|--------|---------|--------|--------|--------|--------|---------|--------|---------|--------|-------|-------|--------|------|------|------|--|
| | 15 | 21 | 22 | 23 | 24 | 25 | 31 | 32 | 33 | 34 | 35 | 2 | 4 | 5 | 6 | 7 | 8 | | | | |
| SiO ₂ | 60.87 | 63.65 | 59.91 | 58.15 | 63.67 | 65.11 | 64.99 | 62.57 | 66.74 | 64.75 | 66.04 | 58.45 | 58.74 | 58.45 | 59.36 | 58.24 | 58.74 | | | | |
| Al ₂ O ₃ | 25.32 | 24.00 | 26.53 | 27.29 | 24.48 | 23.35 | 23.18 | 24.94 | 22.99 | 23.20 | 22.76 | 25.90 | 26.34 | 26.54 | 26.03 | 26.66 | 27.26 | | | | |
| K ₂ O | 0.04 | 0.05 | 0.03 | 0.04 | 0.05 | 0.04 | 0.04 | 0.06 | 0.06 | 0.06 | 0.05 | 0.06 | 0.05 | 0.05 | 0.04 | 0.04 | 0.04 | 0.04 | 0.04 | 0.04 | |
| MnO | 0.01 | 0.00 | 0.00 | 0.01 | 0.00 | 0.00 | 0.00 | 0.01 | 0.00 | 0.00 | 0.00 | 0.00 | 0.00 | 0.01 | 0.00 | 0.00 | 0.00 | 0.00 | 0.00 | 0.00 | |
| TiO ₂ | 0.00 | 0.01 | 0.00 | 0.00 | 0.02 | 0.00 | 0.00 | 0.01 | 0.00 | 0.00 | 0.00 | 0.00 | 0.00 | 0.00 | 0.00 | 0.01 | 0.00 | 0.00 | 0.00 | 0.01 | |
| CaO | 6.38 | 4.54 | 7.22 | 8.68 | 4.70 | 3.43 | 3.49 | 5.36 | 3.48 | 3.56 | 2.94 | 7.54 | 7.59 | 8.18 | 7.36 | 8.12 | 8.26 | | | | |
| Na ₂ O | 7.10 | 8.44 | 6.55 | 6.10 | 7.92 | 8.76 | 8.89 | 7.85 | 7.64 | 8.72 | 8.83 | 6.83 | 6.75 | 6.32 | 6.83 | 6.43 | 6.26 | | | | |
| MgO | 0.01 | 0.00 | 0.00 | 0.00 | 0.01 | 0.00 | 0.00 | 0.00 | 0.01 | 0.01 | 0.00 | 0.01 | 0.01 | 0.00 | 0.00 | 0.01 | 0.00 | 0.01 | 0.00 | 0.00 | |
| TFeO | 0.09 | 0.07 | 0.07 | 0.15 | 0.08 | 0.09 | 0.08 | 0.11 | 0.06 | 0.13 | 0.07 | 0.16 | 0.10 | 0.11 | 0.07 | 0.05 | 0.08 | | | | |
| 总计 | 99.82 | 100.80 | 100.38 | 100.44 | 100.96 | 100.79 | 100.68 | 100.94 | 101.01 | 100.44 | 100.75 | 99.78 | 99.61 | 99.70 | 99.71 | 99.55 | 100.67 | | | | |
| Si | 10.81 | 11.14 | 10.49 | 10.18 | 11.14 | 11.40 | 11.37 | 10.95 | 11.68 | 11.33 | 11.56 | 10.53 | 10.59 | 10.53 | 10.70 | 10.50 | 10.59 | | | | |
| Al | 5.30 | 4.95 | 5.47 | 5.63 | 5.05 | 4.82 | 4.78 | 5.14 | 4.74 | 4.78 | 4.69 | 5.50 | 5.59 | 5.64 | 5.53 | 5.66 | 5.79 | | | | |
| Fe | 0.01 | 0.01 | 0.01 | 0.02 | 0.01 | 0.01 | 0.01 | 0.02 | 0.01 | 0.02 | 0.01 | 0.02 | 0.01 | 0.02 | 0.01 | 0.01 | 0.01 | 0.01 | 0.01 | 0.01 | |
| Ca | 1.21 | 0.85 | 1.35 | 1.63 | 0.88 | 0.64 | 0.65 | 1.01 | 0.65 | 0.67 | 0.55 | 1.46 | 1.47 | 1.58 | 1.42 | 1.57 | 1.59 | | | | |
| Na | 2.44 | 2.86 | 2.22 | 2.07 | 2.69 | 2.97 | 3.02 | 2.66 | 2.59 | 2.96 | 3.00 | 2.39 | 2.36 | 2.21 | 2.39 | 2.25 | 2.19 | | | | |
| K | 0.01 | 0.01 | 0.01 | 0.01 | 0.01 | 0.01 | 0.01 | 0.01 | 0.01 | 0.01 | 0.01 | 0.01 | 0.01 | 0.01 | 0.01 | 0.01 | 0.01 | 0.01 | 0.01 | 0.01 | |
| 总计 | 19.79 | 19.82 | 19.55 | 19.53 | 19.79 | 19.85 | 19.85 | 19.79 | 19.69 | 19.77 | 19.82 | 19.91 | 20.03 | 19.98 | 20.05 | 19.99 | 20.18 | | | | |
| An | 33.10 | 22.86 | 37.79 | 43.94 | 24.61 | 17.73 | 17.77 | 27.33 | 20.03 | 18.32 | 15.50 | 37.78 | 38.22 | 41.57 | 37.24 | 41.01 | 42.06 | | | | |
| Ab | 66.67 | 76.86 | 62.03 | 55.85 | 75.06 | 82.03 | 81.97 | 72.33 | 79.56 | 81.32 | 84.18 | 61.87 | 61.49 | 58.11 | 62.54 | 58.78 | 57.68 | | | | |
| Or | 0.23 | 0.28 | 0.18 | 0.21 | 0.34 | 0.24 | 0.26 | 0.34 | 0.41 | 0.36 | 0.33 | 0.35 | 0.29 | 0.32 | 0.22 | 0.21 | 0.25 | | | | |
| 端元 | 中长石 | 奥长石 | 中长石 | 中长石 | 奥长石 | 奥长石 | 奥长石 | 奥长石 | 奥长石 | 奥长石 | 奥长石 | 中长石 | 中长石 | 中长石 | 中长石 | 中长石 | 中长石 | | | | |
| 样品号 | SD203-3 | | | | | SD204-2 | | | | | SD204-3 | | | | | | | | | | |
| 测点号 | 9 | 10 | 21 | 22 | 25 | 21 | 22 | 23 | 24 | 25 | 6 | 7 | 8 | 9 | 10 | | | | | | |
| SiO ₂ | 59.08 | 59.68 | 60.08 | 58.50 | 62.39 | 57.90 | 56.20 | 58.15 | 57.48 | 58.11 | 59.10 | 58.92 | 59.37 | 59.85 | 58.97 | | | | | | |
| Al ₂ O ₃ | 26.90 | 26.98 | 25.75 | 27.11 | 24.63 | 26.85 | 26.86 | 26.11 | 27.16 | 26.27 | 26.22 | 27.67 | 26.55 | 27.45 | 25.97 | | | | | | |
| K ₂ O | 0.04 | 0.03 | 0.05 | 0.03 | 0.04 | 0.07 | 0.05 | 0.06 | 0.06 | 0.05 | 0.04 | 0.03 | 0.04 | 0.02 | 0.05 | | | | | | |
| MnO | 0.01 | 0.00 | 0.02 | 0.00 | 0.03 | 0.01 | 0.01 | 0.00 | 0.00 | 0.01 | 0.00 | 0.00 | 0.00 | 0.00 | 0.02 | | | | | | |
| TiO ₂ | 0.00 | 0.00 | 0.00 | 0.00 | 0.00 | 0.00 | 0.00 | 0.00 | 0.00 | 0.00 | 0.00 | 0.00 | 0.00 | 0.00 | 0.00 | | | | | | |
| CaO | 7.96 | 7.68 | 7.09 | 8.45 | 5.21 | 8.46 | 8.33 | 7.84 | 8.60 | 7.87 | 7.66 | 8.63 | 7.62 | 7.86 | 7.54 | | | | | | |
| Na ₂ O | 6.34 | 6.20 | 6.94 | 6.24 | 7.79 | 6.14 | 6.21 | 6.36 | 6.00 | 6.41 | 6.84 | 6.33 | 6.68 | 6.49 | 6.72 | | | | | | |
| MgO | 0.00 | 0.00 | 0.01 | 0.00 | 0.01 | 0.00 | 0.00 | 0.01 | 0.00 | 0.00 | 0.00 | 0.00 | 0.00 | 0.01 | 0.00 | | | | | | |
| TFeO | 0.06 | 0.11 | 0.11 | 0.13 | 0.08 | 0.13 | 0.09 | 0.18 | 0.19 | 0.15 | 0.14 | 0.14 | 0.10 | 0.13 | 0.17 | | | | | | |
| 总计 | 100.39 | 100.76 | 100.07 | 100.47 | 100.18 | 99.60 | 97.77 | 98.75 | 99.50 | 98.90 | 100.03 | 101.76 | 100.39 | 101.84 | 99.45 | | | | | | |
| Si | 10.65 | 10.75 | 10.83 | 10.54 | 11.24 | 10.39 | 10.08 | 10.43 | 10.31 | 10.42 | 10.60 | 10.57 | 10.65 | 10.73 | 10.58 | | | | | | |
| Al | 5.71 | 5.73 | 5.47 | 5.76 | 5.23 | 5.67 | 5.68 | 5.52 | 5.74 | 5.55 | 5.54 | 5.85 | 5.61 | 5.80 | 5.49 | | | | | | |
| Fe | 0.01 | 0.02 | 0.02 | 0.02 | 0.01 | 0.02 | 0.01 | 0.03 | 0.03 | 0.02 | 0.02 | 0.02 | 0.01 | 0.02 | 0.03 | | | | | | |
| Ca | 1.54 | 1.48 | 1.37 | 1.63 | 1.01 | 1.63 | 1.60 | 1.51 | 1.65 | 1.51 | 1.47 | 1.66 | 1.46 | 1.51 | 1.45 | | | | | | |
| Na | 2.21 | 2.16 | 2.42 | 2.18 | 2.72 | 2.13 | 2.16 | 2.21 | 2.09 | 2.23 | 2.38 | 2.20 | 2.32 | 2.26 | 2.34 | | | | | | |
| K | 0.01 | 0.01 | 0.01 | 0.01 | 0.01 | 0.01 | 0.01 | 0.01 | 0.01 | 0.01 | 0.01 | 0.01 | 0.01 | 0.01 | 0.01 | | | | | | |
| 总计 | 20.13 | 20.16 | 20.12 | 20.14 | 20.22 | 19.85 | 19.54 | 19.71 | 19.83 | 19.75 | 20.02 | 20.30 | 20.07 | 20.33 | 19.89 | | | | | | |
| An | 40.90 | 40.58 | 35.98 | 42.71 | 26.92 | 43.06 | 42.45 | 40.39 | 44.01 | 40.31 | 38.15 | 42.87 | 38.56 | 40.03 | 38.17 | | | | | | |
| Ab | 58.88 | 59.22 | 63.72 | 57.08 | 72.85 | 56.55 | 57.24 | 59.27 | 55.62 | 59.41 | 61.64 | 56.97 | 61.22 | 59.83 | 61.55 | | | | | | |
| Or | 0.23 | 0.20 | 0.31 | 0.20 | 0.23 | 0.39 | 0.31 | 0.34 | 0.37 | 0.28 | 0.21 | 0.16 | 0.22 | 0.15 | 0.28 | | | | | | |
| 端元 | 中长石 | 中长石 | 中长石 | 中长石 | 中长石 | 奥长石 | 中长石 | 中长石 | 中长石 | 中长石 | 中长石 | 中长石 | 中长石 | 中长石 | 中长石 | 中长石 | 中长石 | 中长石 | 中长石 | 中长石 | |

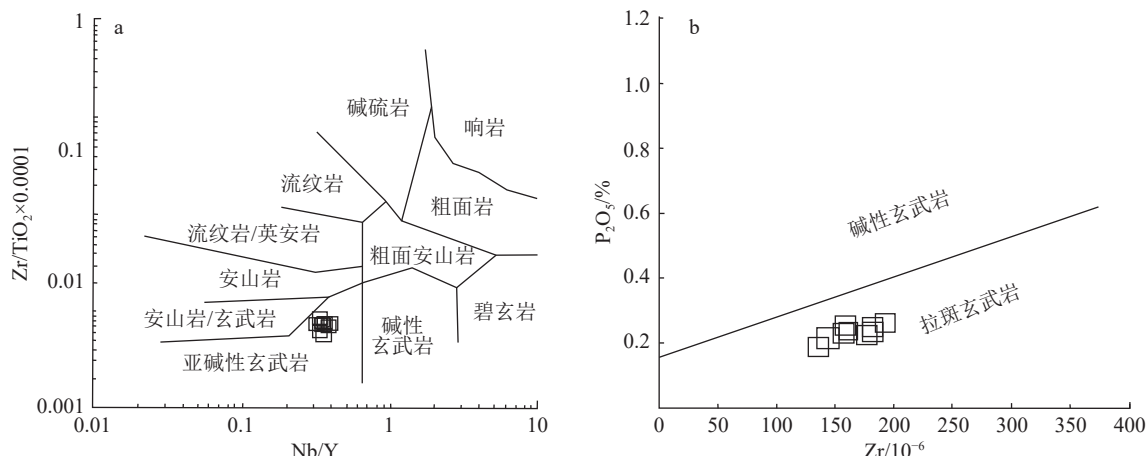
注:以6个O原子为基准计算的阳离子

表5 赣南上洞变玄武岩主量元素分析结果

Table 5 Analysis results of major elements for the meta-basalt from Shangdong, southern Jiangxi

%

| 样品号 | SD201 | SD202 | SD203 | SD204 | SD205 | SD206 | SD207 | SD208 | SD209 |
|---------------------------------|-------|-------|-------|-------|-------|-------|-------|-------|-------|
| SiO ₂ | 48.33 | 48.06 | 47.45 | 49.17 | 48.85 | 49.49 | 49.33 | 48.40 | 48.89 |
| Al ₂ O ₃ | 14.05 | 14.46 | 14.31 | 14.14 | 14.09 | 14.59 | 14.45 | 14.24 | 14.05 |
| MgO | 6.01 | 5.83 | 6.06 | 5.75 | 5.80 | 5.37 | 5.53 | 5.90 | 6.33 |
| Na ₂ O | 2.84 | 2.82 | 2.69 | 2.59 | 2.52 | 2.61 | 2.23 | 3.01 | 2.85 |
| K ₂ O | 0.38 | 0.43 | 0.43 | 0.25 | 0.24 | 0.24 | 0.27 | 0.38 | 0.20 |
| P ₂ O ₅ | 0.24 | 0.24 | 0.25 | 0.24 | 0.24 | 0.27 | 0.25 | 0.22 | 0.20 |
| TiO ₂ | 2.35 | 2.37 | 2.39 | 2.39 | 2.39 | 2.24 | 2.19 | 2.34 | 2.14 |
| CaO | 9.73 | 10.04 | 10.06 | 9.98 | 10.09 | 9.93 | 10.73 | 9.71 | 10.53 |
| TFe ₂ O ₃ | 14.73 | 14.46 | 14.95 | 14.39 | 14.39 | 14.11 | 13.78 | 14.75 | 13.71 |
| MnO | 0.21 | 0.21 | 0.22 | 0.21 | 0.21 | 0.20 | 0.20 | 0.20 | 0.20 |
| Mg [#] | 42.09 | 41.80 | 41.93 | 41.62 | 41.81 | 40.44 | 41.71 | 41.60 | 45.16 |
| 烧失量 | 0.52 | 0.70 | 0.53 | 0.59 | 0.57 | 0.47 | 0.48 | 0.46 | 0.48 |
| 总计 | 99.41 | 99.63 | 99.34 | 99.69 | 99.38 | 99.52 | 99.44 | 99.62 | 99.58 |

注: Mg[#]=100×Mg/(Mg+Fe²⁺)图8 火山岩 Nb/Y-Zr/TiO₂×0.0001 岩石化学分类图解(a, 周岱等, 2017) 和
玄武岩 Zr-P₂O₅ 判别图解(b, Winchester and Floyd, 1976)Fig. 8 Volcanic rock Nb/Y-Zr/TiO₂×0.0001 geochemical classification diagram (a) and basalt Zr-P₂O₅ discrimination diagram (b)

$T(^{\circ}\text{C})=1056.8986+902.7978\text{Al}$ (Al, 以6个氧原子计算阳离子数)。对研究区变玄武岩中单斜辉石的结晶温压进行估算, 结晶温度为114~1246℃(平均1184℃)。黑云母 Fe²⁺-Fe³⁺-Mg²⁺图解(图11-a)中变玄武岩黑云母投点于较高的氧逸度环境(Wones, 1989)。同时, 黑云母的高钛和结构式中低 Al^{VI}值也指示其形成于相对高温和较高氧逸度的条件(Buddington, 1964; Albuquerque, 1973)。在 Ti-Mg/(Mg+Fe)图解(图11-b)中, 变玄武岩中黑云母

的结晶温度为645~675℃(平均660℃)。利用钙质角闪石Ti温度计($T(^{\circ}\text{C})=389+5098.36\text{Ti}$ ($\text{Ti}<0.054$))估算得出的角闪石形成温度为542~675℃(平均594℃)(Gerya et al., 1997)。综上可以推断, 变玄武岩形成于高温、高氧逸度的环境。

4.2 岩石成因

斜长石的分离结晶或岩浆源区残留斜长石会导致Eu、Sr、Ba表现出类似的亏损特征。变玄武岩样品遭受了相当程度的蚀变作用, 显著的负Sr异常而

表 6 赣南上洞变玄武岩稀土和微量元素分析结果测试数据

Table 6 Analysis results of rare earth elements and trace elements in
the Shangdong meta-basalt, Southern Jiangxi 10^{-6}

| 元素 | SD201 | SD202 | SD203 | SD204 | SD205 | SD206 | SD207 | SD208 | SD209 |
|----|----------|----------|----------|----------|----------|----------|----------|----------|----------|
| Li | 35.38 | 40.94 | 35.27 | 38.61 | 43.66 | 48.88 | 44.08 | 51.19 | 32.02 |
| Be | 0.90 | 0.81 | 0.78 | 0.93 | 0.91 | 1.03 | 1.09 | 0.80 | 0.73 |
| Sc | 38.49 | 37.24 | 38.67 | 38.26 | 37.46 | 35.36 | 35.70 | 37.98 | 40.05 |
| Ti | 14338.44 | 14148.33 | 14108.69 | 14475.53 | 14308.72 | 13204.30 | 12999.82 | 14008.60 | 12773.29 |
| V | 340.93 | 321.51 | 326.29 | 342.59 | 338.60 | 322.67 | 314.12 | 367.51 | 332.18 |
| Cr | 70.96 | 68.73 | 74.19 | 79.14 | 68.24 | 57.77 | 62.42 | 60.11 | 90.28 |
| Mn | 1708.11 | 1689.67 | 1725.69 | 1738.04 | 1735.50 | 1632.46 | 1671.34 | 1639.71 | 1635.38 |
| Co | 44.91 | 43.26 | 44.91 | 44.87 | 45.30 | 42.15 | 41.36 | 44.36 | 44.93 |
| Ni | 43.51 | 41.56 | 41.96 | 48.57 | 45.11 | 39.46 | 40.93 | 47.02 | 51.84 |
| Cu | 53.41 | 55.91 | 47.90 | 71.31 | 65.91 | 65.53 | 59.49 | 92.60 | 63.99 |
| Zn | 126.06 | 121.42 | 126.54 | 127.00 | 123.30 | 120.38 | 114.27 | 117.74 | 110.26 |
| Ga | 20.78 | 20.67 | 20.69 | 21.79 | 21.55 | 22.15 | 23.02 | 20.89 | 19.89 |
| Rb | 38.12 | 42.44 | 41.40 | 14.19 | 13.29 | 14.08 | 20.99 | 27.66 | 7.18 |
| Sr | 241.92 | 245.27 | 234.00 | 255.28 | 254.61 | 262.56 | 250.01 | 266.26 | 188.66 |
| Y | 32.94 | 32.87 | 34.01 | 34.60 | 34.61 | 36.55 | 35.42 | 30.61 | 29.00 |
| Zr | 159.03 | 155.99 | 157.02 | 177.93 | 174.48 | 189.97 | 179.03 | 140.25 | 134.62 |
| Nb | 11.38 | 11.43 | 11.51 | 12.43 | 12.08 | 12.88 | 12.51 | 10.37 | 9.51 |
| Mo | 0.73 | 0.74 | 0.64 | 1.01 | 0.85 | 0.74 | 0.71 | 0.59 | 0.89 |
| Sn | 1.38 | 1.29 | 1.28 | 1.63 | 1.65 | 1.64 | 1.75 | 1.14 | 1.17 |
| Cs | 48.25 | 23.55 | 58.69 | 24.92 | 11.41 | 19.32 | 5.54 | 61.42 | 5.22 |
| Ba | 95.86 | 94.51 | 109.74 | 62.74 | 67.57 | 62.87 | 50.30 | 100.26 | 30.17 |
| Hf | 3.85 | 3.81 | 3.82 | 4.29 | 4.23 | 4.54 | 4.33 | 3.45 | 3.31 |
| Ta | 0.64 | 0.64 | 0.64 | 0.70 | 0.69 | 0.73 | 0.70 | 0.57 | 0.53 |
| W | 0.64 | 0.88 | 0.54 | 0.59 | 0.46 | 0.48 | 0.78 | 0.79 | 0.69 |
| Tl | 0.29 | 0.28 | 0.27 | 0.19 | 0.14 | 0.14 | 0.19 | 0.21 | 0.10 |
| Pb | 1.82 | 1.72 | 1.46 | 2.02 | 2.04 | 2.01 | 1.83 | 1.90 | 2.12 |
| Th | 1.31 | 1.29 | 1.29 | 1.46 | 1.44 | 1.55 | 1.47 | 1.13 | 1.01 |
| U | 0.38 | 0.40 | 0.39 | 0.44 | 0.42 | 0.44 | 0.43 | 0.32 | 0.29 |
| La | 11.11 | 11.20 | 11.32 | 12.27 | 12.19 | 12.94 | 12.85 | 10.37 | 9.23 |
| Ce | 26.71 | 27.10 | 27.19 | 29.68 | 29.34 | 31.25 | 30.65 | 24.87 | 22.18 |
| Pr | 4.06 | 4.10 | 4.14 | 4.43 | 4.42 | 4.72 | 4.57 | 3.77 | 3.41 |
| Nd | 19.13 | 19.23 | 19.66 | 20.81 | 20.68 | 21.98 | 21.20 | 17.91 | 16.09 |
| Sm | 5.15 | 5.15 | 5.32 | 5.55 | 5.51 | 5.85 | 5.67 | 4.88 | 4.45 |
| Eu | 1.88 | 1.93 | 1.96 | 2.03 | 1.98 | 2.07 | 2.16 | 1.85 | 1.72 |
| Gd | 5.76 | 5.75 | 5.90 | 6.12 | 6.10 | 6.41 | 6.27 | 5.47 | 5.06 |
| Tb | 0.97 | 0.97 | 1.00 | 1.03 | 1.03 | 1.09 | 1.06 | 0.92 | 0.86 |
| Dy | 5.79 | 5.77 | 5.94 | 6.16 | 6.18 | 6.54 | 6.39 | 5.50 | 5.20 |
| Ho | 1.18 | 1.19 | 1.21 | 1.26 | 1.26 | 1.33 | 1.30 | 1.12 | 1.07 |
| Er | 3.37 | 3.37 | 3.44 | 3.61 | 3.59 | 3.79 | 3.68 | 3.16 | 3.02 |
| Tm | 0.45 | 0.45 | 0.46 | 0.48 | 0.48 | 0.51 | 0.50 | 0.42 | 0.41 |
| Yb | 2.84 | 2.79 | 2.85 | 3.04 | 3.06 | 3.21 | 3.11 | 2.63 | 2.53 |
| Lu | 0.42 | 0.42 | 0.42 | 0.45 | 0.45 | 0.47 | 0.46 | 0.39 | 0.38 |

续表 6

| 元素 | SD201 | SD202 | SD203 | SD204 | SD205 | SD206 | SD207 | SD208 | SD209 |
|----------------------|-------|-------|-------|-------|-------|--------|-------|-------|-------|
| Σ REE | 88.82 | 89.40 | 90.80 | 96.93 | 96.28 | 102.17 | 99.86 | 83.28 | 75.61 |
| Σ LREE | 68.03 | 68.71 | 69.59 | 74.77 | 74.13 | 78.81 | 77.10 | 63.66 | 57.08 |
| Σ HREE | 20.79 | 20.69 | 21.21 | 22.16 | 22.15 | 23.36 | 22.76 | 19.62 | 18.53 |
| LREE/HREE | 3.27 | 3.32 | 3.28 | 3.37 | 3.35 | 3.37 | 3.39 | 3.25 | 3.08 |
| (La/Yb) _N | 2.66 | 2.73 | 2.70 | 2.75 | 2.71 | 2.74 | 2.81 | 2.68 | 2.48 |
| (La/Sm) _N | 1.35 | 1.36 | 1.33 | 1.38 | 1.38 | 1.38 | 1.41 | 1.33 | 1.30 |
| La/Yb | 3.91 | 4.01 | 3.98 | 4.04 | 3.99 | 4.03 | 4.13 | 3.95 | 3.64 |
| δ Eu | 1.05 | 1.08 | 1.06 | 1.06 | 1.04 | 1.03 | 1.11 | 1.09 | 1.10 |
| δ Ce | 0.96 | 0.96 | 0.95 | 0.97 | 0.96 | 0.96 | 0.96 | 0.96 | 0.95 |

注: δ Eu=Eu/Eu*-Eu_N/((Sm_N+Gd_N)/2)

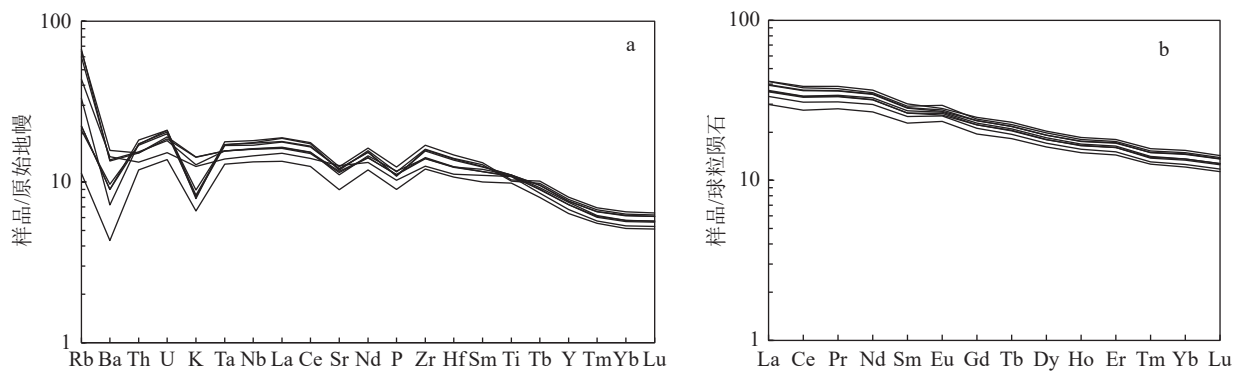


图 9 原始地幔标准化微量元素蛛网图 (a) 和球粒陨石标准化稀土元素配分图 (b)(标准化值据 Sun and McDonough, 1989)

Fig. 9 Spider diagrams of trace elements normalized to primitive mantle (a) and standardized rare earth element distribution diagrams for chondrite (b)

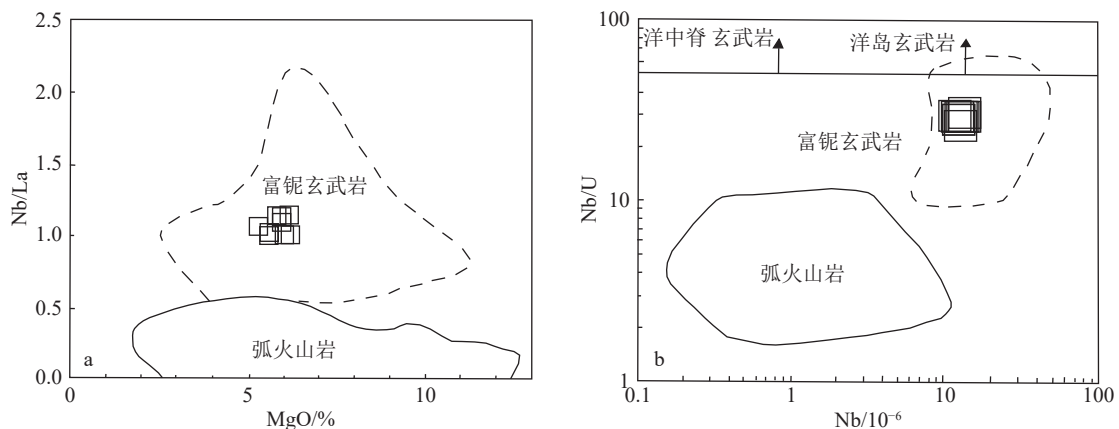


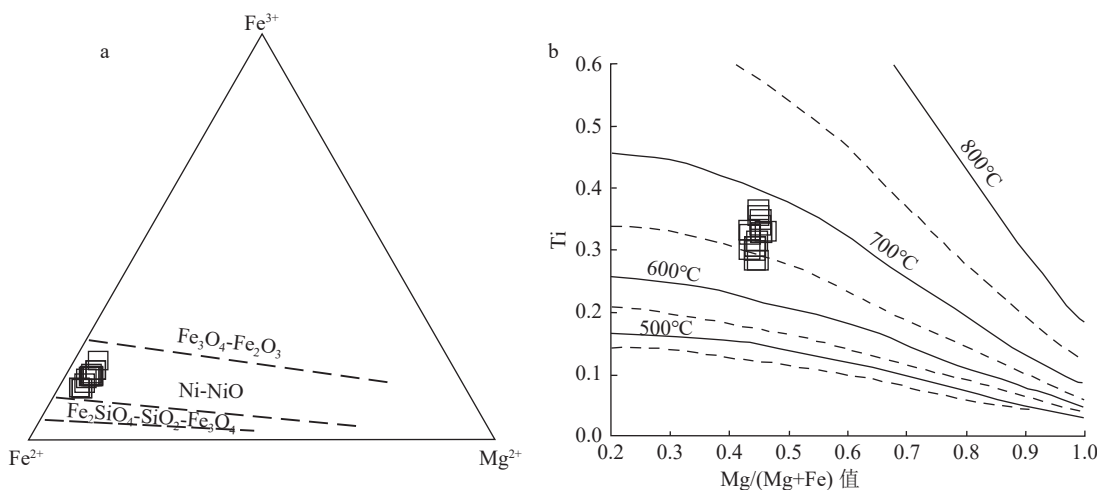
图 10 玄武岩 MgO-Nb/La(a) 和 Nb-Nb/U(b) 图解 (据 Kepezhinskis et al., 1996)

Fig. 10 Diagrams of MgO-Nb/La (a) and Nb-Nb/U (b) in basalt

没有负 Eu 异常 (图 9), 表明岩浆未发生显著的斜长石分离结晶或源区无斜长石的残留, 因而负 Sr 异常和 Rb、Ba 含量较大的变化应该是蚀变作用的结果。

岩浆演化过程中, 分离结晶和同化混染作用往往相伴相生, 即 AFC 过程 (DePaolo, 1981)。变玄武

岩的 La/Sm 值介于 2.07~2.27 之间, 平均为 2.17; (Th/Yb)_{PM} 值为 2.31~2.80, 平均为 2.65, 高的 La/Sm 值 (>4.5) 和 (Th/Yb)_{PM} 值 (>4.6) 指示地壳物质的混染 (Lassiter and DePaolo, 1997; Wang and Zhou, 2008), 表明岩浆侵位过程中不存在地壳物质的混染。高的

图 11 黑云母 Fe^{2+} - Fe^{3+} - Mg^{2+} 图解 (a, 据 Wones, 1989) 和 $\text{Ti}-\text{Mg}/(\text{Mg}+\text{Fe})$ 图解 (b, 据 Henry et al., 2005)Fig. 11 Diagrams of Fe^{2+} - Fe^{3+} - Mg^{2+} (a) and $\text{Ti}-\text{Mg}/(\text{Mg}+\text{Fe})$ (b) of biotite

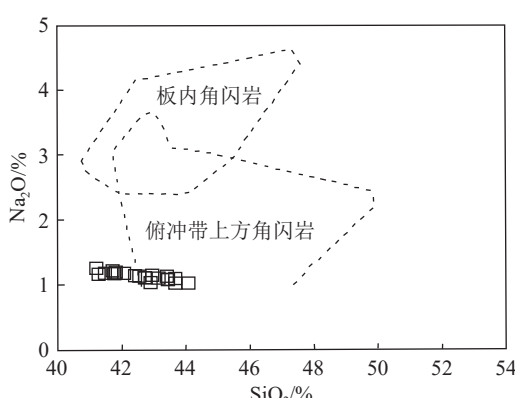
Nb/La 、 Nb/U 值类似于典型的富 Nb 玄武岩 (图 10) (Kepezhinskas et al., 1996; Kepezhinskas and Defant, 1996; 张海祥, 2005), 暗示变玄武岩可能形成于俯冲环境。在角闪石的 $\text{SiO}_2-\text{Na}_2\text{O}$ 图解 (图 12) 中, 投点落入俯冲带上方的角闪石区域, 反映其形成于俯冲带之上的地幔楔, 即角闪石与地幔楔岩浆演化有成因联系 (Coltorti et al., 2007), 因此, 上洞变玄武岩形成于俯冲构造背景。

火成岩中的 Si 与 Al 有互不相容的作用, 可作为确定母岩浆类型的标型元素 (孙传敏, 1994)。单斜辉石在 Si-Al^{IV} 图上大部分落入亚碱性拉斑玄武岩区 (图 4), 与地球化学特征指示岩石系列一致, 指示上洞变玄武岩的母岩浆应为玄武质岩浆。上洞变玄武岩中钙质角闪石的 Al_2O_3 含量为 9.70%~13.86%, $\text{Si}/(\text{Si}+\text{Ti}+\text{Al})$ 值 0.757~0.796, 根据幔源角闪石

Al_2O_3 通常大于 10%, 壳源通常小于 10%; 幔源角闪石结构式中 $\text{Si}/(\text{Si}+\text{Ti}+\text{Al}) \leq 0.765$, 而壳源大于 0.765 (姜常义等, 1984), 显示壳幔混源特征。根据 $\text{MgO}-\text{TFeO}/(\text{TFeO}+\text{MgO})$ 图解 (图 13-a) 区分不同来源的黑云母, 结果显示, 变玄武岩黑云母的数据点位于壳幔混合源区。同时, 在角闪石 $\text{Mg}-\text{Ca}-(\text{Fe}^{2+}+\text{Fe}^{3+})$ 成因判别图解 (图 13-b) 中, 样品也位于壳幔混合源区域。可见, 成岩物质来源具有壳幔混源的特征。

4.3 构造环境

单斜辉石作为镁铁质岩石中最主要的造岩矿物之一, 其矿物化学特征记录了与岩浆起源及构造背景有关的信息, 可为构造-岩浆活动提供重要证据 (Nisbet and Pearce, 1977; Leterrier et al., 1982)。本次研究基于 Nisbet and Pearce(1977) 提出的单斜辉石 F1-F2 图解法, 对研究区火山岩样品的构造环境进行判定。变玄武岩样品点主要分布在火山岛弧玄武岩和洋底玄武岩 (VAB+OFB) 区域 (图 14-a), 部分样品点则位于洋底玄武岩与板块内拉斑玄武岩的交界处。由于岩浆的快速冷却, TiO_2 和 Al_2O_3 含量的富集导致 F2 值偏低, 若排除这一影响, 单斜辉石的投点将向上移动, 更倾向于火山弧玄武岩区域。结合全岩地球化学特征, 在玄武岩 $\text{Th}-\text{Hf}/3-\text{Nb}/6$ 构造环境判别图解 (图 14-b) 中, 所有岩石样品点均位于火山弧玄武岩区。表明矿物学和地球化学特征一致指示上洞变玄武岩形成的构造环境为火山岛弧环境。在华夏加里东褶皱带南缘最新发现变玄武岩, 结合

图 12 角闪石 $\text{SiO}_2-\text{Na}_2\text{O}$ 图解 (据 Coltorti et al., 2007)Fig. 12 $\text{SiO}_2-\text{Na}_2\text{O}$ diagram of hornblende

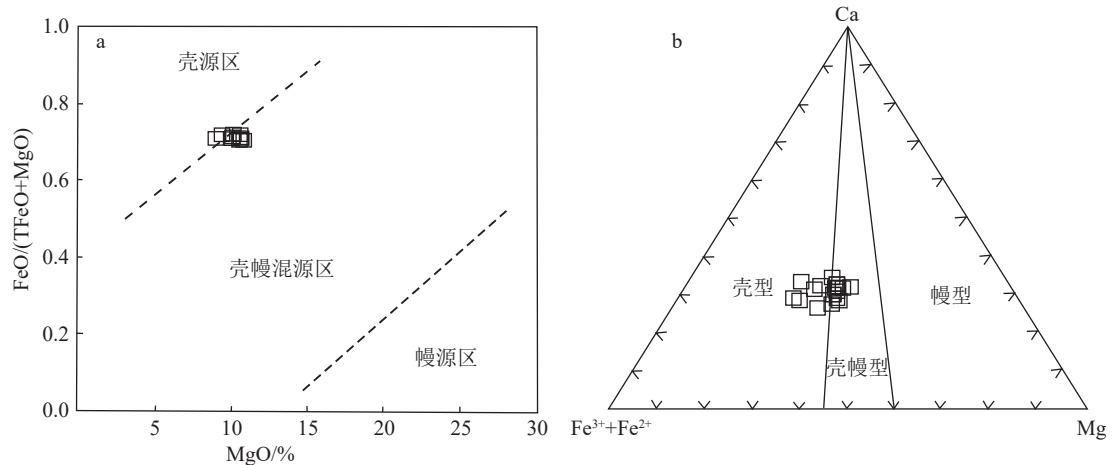


图 13 黑云母 $MgO-TFeO/(TFeO+MgO)$ 图解 (a, 据周作侠, 1988) 和
角闪石 $Ca-(Fe^{2+}+Fe^{3+})-Mg$ 图解 (b, 据谢应雯和张玉泉, 1990)

Fig. 13 Plots of $MgO-TFeO/(TFeO+MgO)$ (a) and $Ca-(Fe^{2+}+Fe^{3+})-Mg$ (b) of the biotite

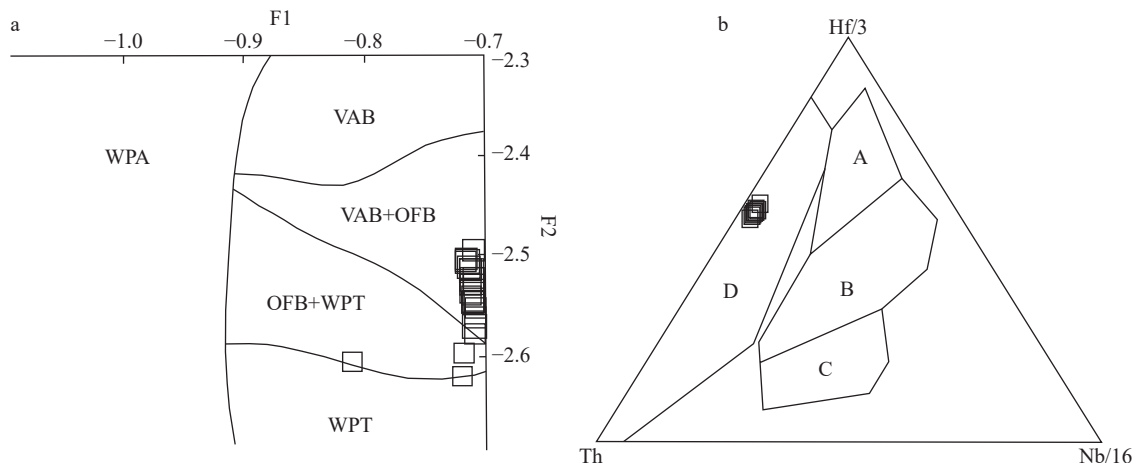


图 14 玄武岩中单斜辉石 F1-F2 图解 (a, 据 Nisbet and Pearce, 1977) 和玄武岩 Th-Hf/3-Nb/6 判别图解 (b, 据 Wood, 1979)

Fig. 14 Graphical representation of clinopyroxene in basalt with F1-F2 classification (a) and Th-Hf/3-Nb/6 discrimination diagram (b) for basaltic rocks

WPT—板块内拉斑玄武岩; WPA—板块内部碱性玄武岩; VAB—火山弧玄武岩; OFB—洋底玄武岩; A—N型 MORB; B—E型 MORB 和板内拉斑玄武岩; C—碱性板内玄武岩; D—火山弧玄武岩

前人研究的变质板岩、安山岩、英安(斑)岩、流纹岩等,无疑为华南地区存在早古生代加里东期洋壳俯冲作用提供了关键证据。虽然目前尚未发现同时期的蛇绿岩,但本文通过对上洞变玄武岩岩石学、矿物学和地球化学的分析,揭示上洞形成于俯冲的岛弧环境,有力地证明华南早古生代加里东期造山运动是板块构造体制下的俯冲背景。

5 结 论

(1) 赣南上洞变玄武岩具富钠 ($NaO=2.23\%$ ~

3.01%)、贫钾 ($K_2O=0.20\% \sim 0.43\%$)、富 Nb 特征,稀土元素总量低,轻、重稀土元素分馏不明显,无明显 Eu 异常,属亚碱性拉斑玄武岩系列;普通辉石 ($Wo_{27 \sim 31}En_{40 \sim 48}Fs_{23 \sim 30}$) 富钙富镁,铁质黑云母富铝、富铁,贫镁、贫钾;普通角闪石富钠、富铝,斜长石 ($An_{16 \sim 44}Ab_{56 \sim 84}$) 贫钛。

(2) 上洞变玄武岩具有壳幔混源特征,变玄武岩的形成与俯冲作用有着密切的关系,形成于结晶温度高、高氧逸度的岛弧环境。结合前人区域研究成果分析认为,扬子板块与华夏板块早古生代可能存在

在古洋盆,形成于岛弧环境的上洞变玄武岩是赣南地区早古生代俯冲背景的地质记录。

References

- Albuquerque A C. 1973. Geochemistry of biotites from granitic rocks, Northern Portugal[J]. *Geochimica et Cosmochimica Acta*, 37(7): 1779–1802.
- Buddington A F, Lindsley D H. 1964. Iron–titanium oxide minerals and synthetic equivalents[J]. *Journal of Petrology*, 5(2): 310–357.
- Cao M X, Zhang D F, Zhang J R, et al. 2025. Genesis of the Chengkeng pluton in south Jiangxi Province during the Early Paleozoic and its geological significance[J]. *Journal of East China University of Technology (Natural Science)*, 48(2): 128–141 (in Chinese with English abstract).
- Charvet J, Shu L, Faure M, et al. 2010. Structural development of the Lower Paleozoic belt of South China: genesis of an intracontinental orogen[J]. *Journal of Asian Earth Sciences*, 39 (4): 309–330.
- Coltorti M, Bonadiman C, Faccini B, et al. 2007. Amphiboles from suprasubduction and intraplate lithospheric mantle[J]. *Lithos*, 99(1): 68–84.
- Deer W A, Howie R A, Zussman J. 1992 . An introduction to the rock forming minerals (2nd Edition)[M]. Harlow: Longman Group: 1–232.
- DePaolo D J. 1981. Trace element and isotopic effects of combined wallrock assimilation and fractional crystallization[J]. *Earth and Planetary Science Letters*, 53(2): 189–202.
- Ding H. 2016. Chronology, geochemical characteristics and petrogenesis of andesites in Nanjing Basin, southern Jiangxi Province[D]. Master's Thesis of East China University of Technology (in Chinese with English abstract).
- Foster M D. 1960. Interpretation of the composition of trioctahedral micas[R].
- Gao P. 2016. Geochemical study of Mesozoic granites in the Nanling region of the South China Block[D]. Ph. D. Dissertation of University of Science and Technology of China (in Chinese with English abstract).
- Gerya T V, Perchuk L L, Triboulet C, et al. 1997. Petrology of the Tumanshet zonal metamorphic complex, eastern Sayan[J]. *Petrology*, 5(6): 503–533.
- Guan Y L, Yuan C, Long X P, et al. 2013. Early Paleozoic intracontinental orogeny in the eastern South China Block: Constraints from I-type granites[J]. *Geotectonica et Metallogenesis*, 37(4): 698–720 (in Chinese with English abstract).
- Henry D J, Guidotti C V, Thomson J A. 2005. The Ti–saturation surface for low-to-medium pressure metapelitic biotites: Implications for geothermometry and Ti–substitution mechanisms[J]. *American Mineralogist*, 90(2/3): 316–328.
- Jiang C Y, An S Y. 1984. On the chemical composition characteristics of calcic amphibole in igneous rocks and its petrological significance[J]. *Journal of Mineralogy and Petrology*, (3): 1–9 (in Chinese with English abstract).
- Jiao W F, Wu Y B, Yang S H, et al. 2009. The oldest basement rock in the Yangtze Craton revealed by zircon U–Pb age and Hf isotope composition[J]. *Science China version D*, 52: 1393–1399.
- Jin S Q. 1991. Compositional Characteristics of Calcic Amphiboles in Different Regional Metamorphic Facies[J]. *Chinese Science Bulletin*, (11): 851–854 (in Chinese with English abstract).
- Kepezhinskis P, Defant M J, Drummond M S. 1996. Progressive enrichment of island arc mantle by melt–peridotite interaction inferred from Kamchatka xenoliths[J]. *Geochimica et Cosmochimica Acta*, 60(7): 1217–1229.
- Kerr A C. 1998. Mineral chemistry of the Mull–Morvern Tertiary lava succession, western Scotland[J]. *Mineralogical Magazine*, 62(3): 295–312.
- Kushiro I. 1960. Si–Al relation in clinopyroxenes from igneous rocks[J]. *American Journal of Science*, 258(8): 548–554.
- Lao Y J. 2017. Geological and geochemical characteristics and geological significance of Caledonian dacite in Nanjing Basin, southern Jiangxi Province[D]. Master's Thesis of East China University of Technology (in Chinese with English abstract).
- Lassiter J C, DePaolo D J. 1997. Plume/lithosphere interaction in the generation of continental and oceanic flood basalts: chemical and isotopic constraints[J]. *Geophysical Monograph–American Geophysical Union*, 100: 335–356.
- Leterrier J, Maury R C, Thonon P, et al. 1982. Clinopyroxene composition as a method of identification of the magmatic affinity of paleovolcanic series[J]. *Earth and Planetary Science Letters*, 59(1): 139–154.
- Li W X, Li X H, Li Z X. 2005. Neoproterozoic bimodal magmatism in the Cathaysia Block of South China and its tectonic significance[J]. *Precambrian Research*, 136(1): 51–66.
- Li X H, Li W X, Li Z X, et al. 2009. Amalgamation between the Yangtze and Cathaysia Blocks in South China: constraints from SHRIMP U–Pb zircon ages, geochemistry and Nd–Hf isotopes of the Shuangxiu volcanic rocks[J]. *Precambrian Research*, 174(1/2): 117–128.
- Li Z X, Li X H, Wartho J A, et al. 2010a. Magmatic and metamorphic events during the early Paleozoic Wuyi–Yunkai orogeny, southeastern South China: New age constraints and pressure–temperature conditions[J]. *GSA Bulletin*, 122(5/6): 772–793.
- Li Z X, Li X H, Wartho J A, et al. 2010b. Magmatic and metamorphic events during the early Paleozoic Wuyi–Yunkai orogeny, southeastern South China: new age constraints and pressure–temperature conditions[J]. *Geological Society of America Bulletin*, 122(5/6): 772–793.
- Liu S, Ma S S, Huang M H, et al. 2020. Geochronology, geochemical characteristics and geological significance of Type I rhyolite in Nanjing Basin, southern Jiangxi Province[J]. *Geochimica*, 49(4): 404–421 (in Chinese with English abstract).
- Liu S, Wu J H, Yang D G, et al. 2021. New evidence for the geological age of the Huangzhudong Formation of the Longtouzhai Group in the middle segment of the Qin-Hang Joint Belt: SHRIMP zircon U–Pb age of rhyolite interlayers and its geological significance[J]. *Acta Petrologica Sinica*, 37(5): 1431–1443 (in Chinese with English abstract).
- Ma S S, Liu S, Huang M H, et al. 2019. U–Pb geochronology, geochemical characteristics and genesis of Miaoyun pluton in southern Jiangxi Province[J]. *Science Technology and Engineering*, 19(26):

- 55–67 (in Chinese with English abstract).
- Morimoto N. 1988. Die Nomenklatur von Pyroxenen [J]. *Mineralogy and Petrology*, 39: 55–76.
- Nachit H, Ibhi A, Ohoud M B. 2005. Discrimination between primary magmatic biotites, reequilibrated biotites and neoformed biotites [J]. *Comptes Rendus Geoscience*, 337(16): 1415–1420.
- Nisbet E G, Pearce J A. 1977. Clinopyroxene composition in mafic lavas from different tectonic settings [J]. *Contributions to Mineralogy and Petrology*, 63(2): 149–160.
- Niu M L, Zhao Q Q, Wu Q, et al. 2018. Magma mixing of the Guokeshan pluton in the northern margin of Qaidam Basin: Evidence from petrography, mineralogy and geochemistry [J]. *Acta Petrologica Sinica*, 34(7): 1991–2016 (in Chinese with English abstract).
- Peng S B, Liu S F, Lin M S, et al. 2016. Early Paleozoic subduction in Cathaysia (II): New evidence from Dashuang high-Mg and magnesian andesites [J]. *Earth Science*, 41(6): 931–947 (in Chinese with English abstract).
- Shu L S. 2012. An analysis of principal features of tectonic evolution in South China Block [J]. *Geological Bulletin of China*, 31(7): 1035–1053 (in Chinese with English abstract).
- Stone D. 2000. Temperature and pressure variations in suites of Archean felsic plutonic rocks, Berens River area, Northwest Superior Province, Ontario, Canada [J]. *The Canadian Mineralogist*, 38(2): 455–470.
- Sun C M. 1994. Genetic mineralogy of pyroxenes from Proterozoic ophiolite in Yanbian, Sichuan and its tectonic significance [J]. *Journal of Mineralogy and Petrology*, 3(1): 1–15 (in Chinese with English abstract).
- Sun S S, McDonough W F. 1989. Chemical and isotopic systematics of oceanic basalts: Implications for mantle composition and processes [J]. Geological Society, London, Special Publications, 42(1): 313–345.
- Thompson R N. 1974. Some high-pressure pyroxenes [J]. *Mineralogical Magazine*, 39(307): 768–787.
- Wang D Z. 2004. Review and perspective on granite research in South China [J]. *Geological Journal of China Universities*, 10(3): 305–314 (in Chinese with English abstract).
- Wang J, Li Z X. 2003. History of Neoproterozoic rift basins in South China implications for Rodinia break-up [J]. *Precambrian Research*, 122: 141–158.
- Wang Q, Xu J F, Jian P, et al. 2006. Petrogenesis of adakitic porphyries in an extensional tectonic setting, Dexing, South China: Implications for the genesis of porphyry copper mineralization [J]. *Journal of Petrology*, 47(1): 119–144.
- Wang Qi L, Zhou M F. 2008. Platinum-group elemental and Sr–Nd–Os isotopic geochemistry of Permian Emeishan flood basalts in Guizhou Province, SW China [J]. *Chemical Geology*, 248(1/2): 83–103.
- Wang S, Tao J H, Li W X, et al. 2004. Zircon U–Pb geochronology, geochemistry and Sr–Nd isotopes of the Maixie pluton in northwestern Jiangxi Province: Implications for petrogenesis [J]. *Acta Geologica Sinica*, 92(4): 747–768 (in Chinese with English abstract).
- Wang Y J, Zhang A M, Fan W M, et al. 2011. Kwangssian crustal anatexis within the eastern South China Block: Geochemical, zircon U–Pb geochronological and Hf isotopic fingerprints from the gneissoid granites of Wugong and Wuyi–Yunkai Domains [J]. *Lithos*, 127(1/2): 239–260.
- Wang Y, Fan W, Zhao G, et al. 2007. Zircon U–Pb geochronology of gneissic rocks in the Yunkai massif and its implications on the Caledonian event in the South China Block [J]. *Gondwana Research*, 12(4): 404–416.
- Winchester J A, Floyd P A. 1976. Geochemical magma type discrimination: application to altered and metamorphosed basic igneous rocks [J]. *Earth and Planetary Science Letters*, 28(3): 459–469.
- Wones D R. 1989. Significance of the assemblage titanite+ magnetite+ quartz in granitic rocks [J]. *American Mineralogist*, 74(7/8): 744–749.
- Wood D A, Joron J L, Treuil M. 1979. A re-appraisal of the use of trace elements to classify and discriminate between magma series erupted in different tectonic settings [J]. *Earth and Planetary Science Letters*, 45(2): 326–336.
- Wu J H, Xiang Y X, Huang G R, et al. 2012. First SHRIMP zircon U–Pb dating of Caledonian porphyroclastic lava in northern Guangdong and its geological significance [J]. *Geological Journal of China Universities*, 18(4): 601–608 (in Chinese with English abstract).
- Wu J, Wang G Q, Liang H Y, et al. 2014. Identification of Caledonian volcanic rocks in the Dabaoshan ore district, northern Guangdong Province and its geological significance [J]. *Acta Petrologica Sinica*, 30(4): 1145–1154 (in Chinese with English abstract).
- Xia Y, Xu X S, Zhu K Y. 2012. Paleoproterozoic S- and A-type granites in southwestern Zhejiang: magmatism, metamorphism and implications for the crustal evolution of the Cathaysia basement [J]. *Precambrian Research*, 216/219: 177–207.
- Xie Y W, Zhang Y Q. 1990. Typomorphic characteristics and genetic significance of amphiboles in granitoids from Hengduan Mountains region [J]. *Acta Mineralogica Sinica*, 10(1): 35–45 (in Chinese with English abstract).
- Xu K Q, Liu Y J, Yu S Y, et al. 1960. Discovery of Caledonian granites in southern Jiangxi [J]. *Geological Review*, 20(3): 112–114 (in Chinese with English abstract).
- Xu X S. 2008. Some problems on the study of granite–volcanic rock genesis in South China [J]. *Geological Journal of China Universities*, 14(3): 283–294 (in Chinese with English abstract).
- Xu Y J, Du Y S, Cawood R A, et al. 2012. Detrital zircon provenance of Upper Ordovician and Silurian strata in the northeastern Yangtze Block: response to orogenesis in South China [J]. *Sedimentary Geology*, 267/268: 63–72.
- Yi L W, Ma C Q, Wang L X, et al. 2014. Discovery of Late Ordovician subvolcanic rocks in South China: Early Paleozoic subduction–related dacites? [J]. *Earth Science (Journal of China University of Geosciences)*, 39(6): 637–653 (in Chinese with English abstract).
- Yu J H, O'Reilly S Y, Wang L J, et al. 2010. Components and episodic growth of Precambrian crust in the Cathaysia Block, south China: Evidence from U–Pb ages and Hf isotopes of zircons in Neoproterozoic sediments [J]. *Precambrian Research*, 181: 97–114.
- Yu J H, O'Reilly S Y, Zhou M F, et al. 2012. U–Pb geochronology and Hf–Nd isotopic geochemistry of the Badu Complex, Southeastern China—Implications for the Precambrian crustal evolution and paleogeography of the Cathaysia Block [J]. *Precambrian Research*, 222–223: 424–449.

- Zhang G W, Guo A L, Wang Y J, et al. 2013. Tectonics of South China continent and its implications [J]. *Science China Earth Sciences*, 56(11): 1804–1828 (in Chinese with English abstract).
- Zhang H X, Zhang B Y, Niu H C. 2005. Nb-enriched basalts: Partial melting products of the mantle wedge metasomatized by slab melt [J]. *Advances in Earth Science*, 20(11): 82–90 (in Chinese with English abstract).
- Zhang S B, Zheng Y F. 2013. Formation and evolution of Precambrian continental lithosphere in South China [J]. *Gondwana Research*, 23(4): 1241–1260.
- Zhang S, Wu J H, Liu S, et al. 2021. Age, genesis of dacite in the Gujiaying Basin, southern Jiangxi Province and its constraints on Early Paleozoic tectonic evolution [J]. *Geological Bulletin of China*, 40(9): 1459–1475 (in Chinese with English abstract).
- Zhang S M, Su T R, Zhu J B, et al. 2024. Zircon Geochronology, Petrogeochemistry and Geological Significance of the Guidong Pluton in the Zhuguangshan Area, South China [J]. *Chinese Journal of Geology*, 59(6): 1722–1747 (in Chinese with English abstract).
- Zheng Y, Zhang S, Zhao Z, et al. 2006. Contrasting zircon Hf and O isotopes in the two episodes of Neoproterozoic granitoids in South China: Implications for growth and reworking of continental crust [J]. *Lithos*, 96(1): 127–150.
- Zhou D, Long W G, Ke X Z, et al. 2017. Petrogenesis of the tectonic melange along the northern margin of Yunkai Massif [J]. *Acta Petrologica Sinica*, 33(3): 810–830 (in Chinese with English abstract).
- Zhou X M, Chen T H, Liu C S, et al. 1982. Pyroxene and amphibole megacrysts in alkali basaltic rocks from the southeastern coast of China [J]. *Acta Mineralogica Sinica*, 2(1): 13–20 (in Chinese with English abstract).
- Zhou X M. 2003. Some thoughts on the study of granites in South China [J]. *Geological Journal of China Universities*, 9(4): 556–565 (in Chinese with English abstract).
- Zhou Z X. 1988. Chemical characteristics of mafic micas in intrusive rocks and their geological significance [J]. *Acta Petrologica Sinica*, 4(3): 63–73 (in Chinese with English abstract).
- Zhu B. 2010. Study on Mantle Fluids and Uranium Mineralization [D]. Ph. D. Dissertation of Chengdu University of Technology (in Chinese with English abstract).
- 附中文参考文献**
- 曹明轩, 张德富, 张健仁, 等. 2025. 赣南早古生代城坑岩体成因及其地质意义 [J]. 东华理工大学学报 (自然科学版), 48(2): 128–141.
- 丁辉. 2016. 江西南部南迳盆地安山岩年代学、地球化学特征及岩石成因 [D]. 东华理工大学硕士学位论文.
- 高彭. 2016. 华南陆块南岭地区中生代花岗岩地球化学研究 [D]. 中国科学技术大学博士学位论文.
- 关义立, 袁超, 龙晓平, 等. 2013. 华南地块东部早古生代的陆内造山作用: 来自 I 型花岗岩的启示 [J]. 大地构造与成矿学, 37(4): 698–720.
- 姜常义, 安三元. 1984. 论火成岩中钙质角闪石的化学组成特征及其岩石学意义 [J]. 矿物岩石, (3): 1–9.
- 靳是琴. 1991. 不同区域变质相中钙质角闪石的成分特征 [J]. 科学通报, (11): 851–854.
- 劳玉军. 2017. 赣南南迳盆地加里东期英安岩地质、地球化学特征及地质意义 [D]. 东华理工大学硕士学位论文.
- 刘帅, 马树松, 黄美化, 等. 2020. 赣南南迳盆地 I 型流纹岩年代学、地球化学特征及其地质意义 [J]. 地球化学, 49(4): 404–421.
- 刘帅, 巫建华, 杨东光, 等. 2021. 钦杭结合带中段龙头寨群黄竹洞组地质时代的新证据: 流纹岩夹层的 SHRIMP 锆石 U-Pb 年龄及地质意义 [J]. 岩石学报, 37(5): 1431–1443.
- 马树松, 刘帅, 黄美化, 等. 2019. 赣南苗云岩体 U-Pb 年代学、地球化学特征及其成因 [J]. 科学技术与工程, 19(26): 55–67.
- 牛漫兰, 赵齐齐, 吴齐, 等. 2018. 柴北缘果可山岩体的岩浆混合作用: 来自岩相学、矿物学和地球化学证据 [J]. 岩石学报, 34(7): 1991–2016.
- 彭松柏, 刘松峰, 林木森, 等. 2016. 华夏早古生代俯冲作用 (II): 大洋高镁-镁质安山岩新证据 [J]. 地球科学, 41(6): 931–947.
- 舒良树. 2012. 华南构造演化的基本特征 [J]. 地质通报, 31(7): 1035–1053.
- 孙传敏. 1994. 四川盐边元古代蛇绿岩中辉石的成因矿物学及其大地构造意义 [J]. 矿物岩石, (3): 1–15.
- 王德滋. 2004. 华南花岗岩研究的回顾与展望 [J]. 高校地质学报, (3): 305–314.
- 王帅, 陶继华, 李武显, 等. 2004. 赣西北麦斜岩体锆石 U-Pb 年代学、地球化学以及 Sr-Nd 同位素研究及其岩石成因 [J]. 地质学报, 92(4): 747–768.
- 巫建华, 项媛馨, 黄国荣, 等. 2012. 广东北部碎斑熔岩加里东期锆石 SHRIMP 年龄的首获及其地质意义 [J]. 高校地质学报, 18(4): 601–608.
- 伍静, 王广强, 梁华英, 等. 2014. 粤北大宝山矿区加里东期火山岩的厘定及其地质意义 [J]. 岩石学报, 30(4): 1145–1154.
- 谢应雯, 张玉泉. 1990. 横断山区花岗岩类中角闪石的标型特征及其成因意义 [J]. 矿物学报, (1): 35–45.
- 徐克勤, 刘英俊, 俞受鳌, 等. 1960. 江西南部加里东期花岗岩的发现 [J]. 地质论评, 20(3): 112–114.
- 徐夕生. 2008. 华南花岗岩-火山岩成因研究的几个问题 [J]. 高校地质学报, (3): 283–294.
- 易立文, 马昌前, 王连训, 等. 2014. 华南晚奥陶世次火山岩的发现: 早古生代与俯冲有关的英安岩? [J]. 地球科学 (中国地质大学学报), 39(6): 637–653.
- 张国伟, 郭安林, 王岳军, 等. 2013. 中国华南大陆构造与问题 [J]. 中国科学: 地球科学, 43(10): 1553–1582.
- 张海祥, 张伯友, 牛贺才. 2005. 富铌玄武岩: 板片熔体交代的地幔楔橄榄岩部分熔融产物 [J]. 地球科学进展, (11): 82–90.
- 张山, 巫建华, 刘帅, 等. 2021. 赣南古家营盆地英安岩时代、成因及对早古生代构造演化的制约 [J]. 地质通报, 40(9): 1459–1475.
- 张素梅, 苏天瑞, 朱俊宾, 等. 2024. 华南诸广山一带桂东岩体年代学、岩石地球化学特征及地质意义 [J]. 地质科学, 59(6): 1722–1747.
- 周岱, 龙文国, 柯贤忠, 等. 2017. 云开地块北缘构造混杂岩的岩石成因探讨 [J]. 岩石学报, 33(3): 810–830.
- 周新民, 陈图华, 刘昌实, 等. 1982. 我国东南沿海碱性玄武质岩石中辉石和角闪石巨晶 [J]. 矿物学报, (1): 13–20.
- 周新民. 2003. 对华南花岗岩研究的若干思考 [J]. 高校地质学报, (4): 556–565.
- 周作侠. 1988. 侵入岩的镁铁云母化学成分特征及其地质意义 [J]. 岩石学报, (3): 63–73.
- 朱捌. 2010. 地幔流体与铀成矿作用研究 [D]. 成都理工大学博士学位论文.